# POLITECNICO DI TORINO

Corso di Laurea Magistrale

in Mechanical Engineering

Tesi di Laurea Magistrale

**Micromobility product development through additive design and manufacturing methods and techniques**


Relatore
Prof. Luca Iuliano

Candidato
Ludovica Chianetta


Dicembre 2020

# Contents

# 1. Introduction

The following paper will show the development of a research study that combines two fields: micromobility and additive manufacturing.
The choice of micromobility as a study subject came from the high influx of micromobility products within the past few years. The demand is still increasing, thus more and more companies are investing capital to develop micromobility devices. To compete with this increasing competitiveness they are adding more features to these devices. In particular, the object of this study is an electric scooter. The quickly expanding field of micromobility has huge implications for the environment, city planning, transportation, and business development and is thus an obvious area of focus.

The choice of additive manufacturing comes from the growth of interest by companies to integrate these innovative technologies into their production and study possible applications in their products. Another influence to study additive manufacturing was the potential it has, especially if combined with the AM optimised design. The design steps are different when compared to components designed for conventional manufacturing techniques and thus this study is crucial for the understanding of the different design approach.
The substantial difference with conventional design is the lack of constraints normally set by standard manufacturing technologies. Undercuts are allowed, complexity of shapes does not influence the cost nor the difficulty of production. The development of additive manufacturing technologies and the design methods associated with it has huge implications on the future of component design, the development cycle, and the manufacturing industry.

As mentioned previously, this study is based on the design of components for an electric scooter. The design expands on the already existing components and adapts them to take advantage of the additive manufacturing process. The components were chosen with the expectation of a reduction in weight and with minimal addition to the cost of production. The components studied were the steering, the fork, the truck and the frame.

The component study involves a re-distribution of the original material, while respecting the few physical constraints constituted by the parts that cannot be modified. The material distribution is aided by the use of a special software, designed for this purpose. The software, with the proper settings and inputs, automatically starts an iterative design cycle. Ideally, the software outputs the most appropriate shape considering the input load conditions, the material selection, and the design goals. The design goals designate some mechanical aspect of the component that needs to be optimised such as mass, stiffness, or thermal conductivity. The software's output is a strong starting point on which the designer will work to make a CAD model. In the case of the study, the most suitable polymer and metal were chosen.
This paper will outline the evaluation of the production process for each component and will consist of the choice of the component's orientation in the machine and evaluation of the feasibility. Finally, an evaluation of the costs related to material and production will be made. This is the final step to choose the most suitable and feasible design.

# 2. Micromobility

The field studied in this thesis is micromobility.

To clarify the study, micromobility must be defined; in general, it is a family of vehicles which have a relatively low weight and speed.
The term “micromobility” was coined by Romanian-American industry analyst Horace H. Dediu, who affirms that the definition is in the word itself. The idea came from the word “microcomputing” – the technological revolution of miniaturising computing devices which began in the ‘60s and became omnipresent by the ‘80s. Following this logic, “micromobility” is derived from the idea of the miniaturisation of the vehicles, which would revolutionise the way of living.

Some of the devices that belong in this group are electric bikes, electric scooters, electric skateboards and to some, even bicycles.
Most of these devices have a characteristic in common: their motion is powered by electricity. Although other sources of power can also be used, like human power, internal combustion engines are excluded from the definition of micromobility vehicles. This distinction is made so that there is association between these devices and revolutionary, clean energy.

Early “ancestors” of micromobility devices can be found as far back as 1655, when the first self-propelling chair, a device that is a cross between a wheel chair and a hand bike, was built by a paraplegic named Stefan Farffler; or in 1733, when an early stroller was developed by William Kent.
The history of micromobility, however, starts with the development of bicycles and scooters. The documented use of these vehicles goes back to 1817, when the “dandy horse”, the first prototype of a bicycle, was introduced in Mannheim, Germany. Only two years after “dandy horse”, the first kick scooter was developed by Denis Johnson. It is a controversial and unclear subject on the matter of who invented the first pedal powered bicycle, nonetheless, they began appearing in documents in the 1860s. The diffusion of both bicycles and scooters became accelerated in the 1880s when people began getting frustrated with the available means of transportation at the time (horses and railroads).
1915 is the year that the “Autoped”, developed by Autoped Company, was invented. The autoped is an early version of a motorised scooter, powered by an air cooled, 4-stroke engine. Their popularity had clearly increased into the usage seen today in modern times but, although revolutionary at their time, can not be classified as micromobility due to their output of greenhouse gasses. In the ‘60s and ‘70s skateboards came into the scene. They quickly became very popular and greatly reduced the popularity and use of scooters.
A new development happened in the 1990s when kick scooters re-gained popularity thanks to their new folding system. In the early 2000s the first electric scooters appeared. Throughout several years the performance of their batteries and motors were developed. As the batteries became lighter and longer lasting and the motors more powerful they began increasing in popularity. A major revolution in micromobility via scooters happened in 2017 when the first dockless electric scooters were offered in big cities. The companies that made this possible were both bicycle sharing and scooter ones. Since 2018, starting in the US, electric scooter sharing became very popular and diffused throughout most major cities.

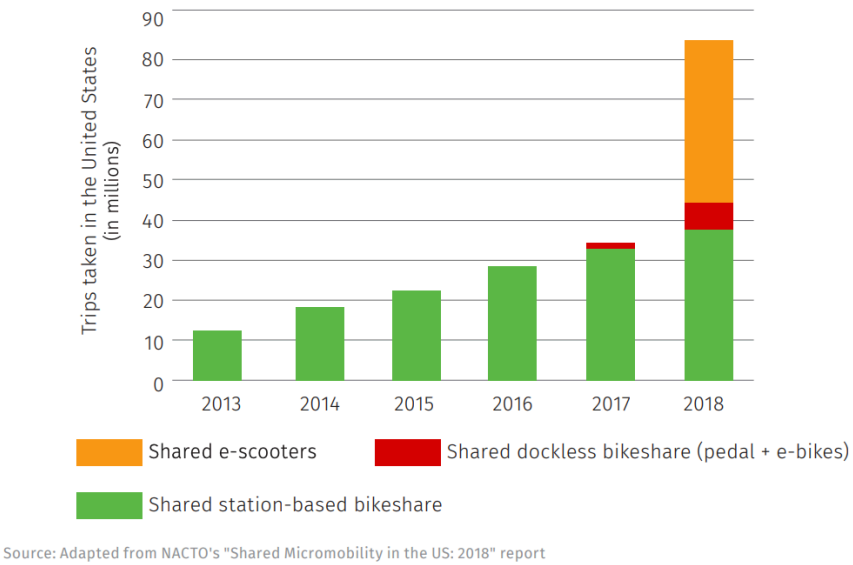


*Figure 2.1: Trips taken in the US with different MB devices from 2013 to 2018*

What is the importance of micromobility?

One of the many important points is the financial accessibility. Compared to more traditional and popular modes of transportation like cars and motorcycles, the difference in price is obvious. Not everyone can easily afford to have a car or a motorcycle, and the cost for smaller electric vehicles is much more sustainable. Moreover, thanks to bike and scooter sharing, the access to this type of transportation became available to a large majority of the population, because there is no need for an initial investment. Instead, for less than a euro per minute charge, the devices can be rented.

Micromobility also has an important implication for the minimisation of environmental pollution. In the past few years air pollution became a recurrent object of conversation and has gained the attention of the popular media. The massive use of internal combustion engines cars has a big influence on the air pollution. The use of bikes, e-bikes, and e-scooters has the potential to greatly reduce the amount of the emissions. It is an important and feasible alternative to travel distances up to 10 kilometres without using the car or public transportation. It is common to travel by foot for up to 2 kilometres . 2 to 7 kilometres can easily be covered by e-scooter and 2 to 10 kilometres can be comfortably traveled by bike.

Another interesting aspect is how lightweight vehicles do not impact the roads and streets as much as heavier vehicles do. As more users use micromobility over traditional transportation methods, less heavy and wearing vehicles are used on the street. This leads to a reduction in the wear of the roads and in the long term will lead to a reduction in the material use and labor costs of re-paving the roads.

Micromobility devices also allow the free passage to limited traffic areas, like in the historical centre of the major cities, where it is very likely that access with cars and motorcycles is

forbidden. This has the potential to greatly decrease one's commute time or allow quick transportation to touristic locations.

Parking is one of the sources of daily stress for those who use traditional means of transport. The low volume of micromobility devices reduces the time spent looking for parking. This is especially the case for e-scooters, which are easy to carry and are usually allowed to be kept at the work place. This is further simplified with the use of shared e-bikes or e-scooters. In the case of docked ones, their stations and availability can be easily found through the brand's app, and are usually well spread out through the city. The dockless ones can be left in any square, sidewalk, or place where there is no transit of vehicles.

If a system were implemented in the streets, similar to bike paths, in order to accommodate an increased number of users, then there will be less cars in traffic. This would lead to higher awareness of the car drivers and micromobility drivers and should ultimately lead to the reduction of pedestrian and cyclists fatalities.

# 3. Additive Manufacturing

Additive manufacturing indicates a typology of production which is based on the addition of material. The method is contrary to the *subtractive manufacturing* method which refers to the more conventional production technologies based on the removal of material in order to obtain parts.
Commonly mistaken with the term “3D printing”, additive manufacturing defines a much broader set of processes. Additive manufacturing can be used to describe the entire process from the use of CAD softwares to create 3D models, the use of a CAM software to read and prepare the file for the machine, and the machine which accepts the CAM output file. After all these steps, the process of additive manufacturing yields the physical part.
The peculiarity of the technology is the way in which the parts are build. The principle of the manufacturing technology is based on the deposition, solidification, and bonding of a thin layer of material, layer by layer, until the desired form is created. The thickness, orientation, and method of deposition of these layers is determined both by the CAM software and the limits of the machine. In most cases the thickness of the layers remains constant throughout the whole part.

The first universally recognised additive manufacturing technology was stereolithography which was developed by Charles Hull and patented in 1984. The method consists of the solidification of a photopolymer activated by means of UV rays. Stereolithography was used only to make prototypes and never as a means for product manufacturing. This was mainly due to the fact that the photopolymers that had to be used with this technology are not recyclable. The invent of stereolithography led to the coining of the term “rapid prototyping”. A prototype is the first iteration of a production series. This technological innovation is revolutionary in the fact that it allows designer to edit a CAD and quickly have the machine print it for each necessary design change. Previously, this process required the designer to manually modify the part or make a new one from scratch using time and labor-intensive additive subtracting methods.
In just three years, rapid prototyping became diffused in the market. In 1990 additive manufacturing techniques were implemented into casting operations; the patterns used to make the moulds for sand foundry were produced for the first time with additive manufacturing. This new method of production took the name “rapid casting”. In five years, AM had developed to the point of allowing what is called “rapid tooling”, where moulds and mould inserts could rapidly be created using AM.
It was finally in the 2000s that the first definitive component was produced with additive technology.
From 2000 on, the number of installed additive manufacturing machines grew exponentially.

Additive manufacturing technologies were developed and implemented mostly for economic reasons. The major factor that influenced the need to develop such technologies was the increased production of short life cycle products. Since the last few decades of the 20$^{th}$ century and even more frequently in the current century, the time it takes an item to enter the market to when it becomes obsolete, has drastically reduced. Due to this trend, companies had to speed up the development times of new or upgraded products in order to remain competitive.

If a company releases a product behind a competitor there may be significant potential profit loss, up to 1/3. Alongside the benefit of speeding up the development phase, additive manufacturing technologies can also potentially help detect and prevent errors during production, which could bring about a 20% profit loss.
However, as previously mentioned, not all the additive manufacturing technologies are used for prototyping. Some machines use the technology to create final products.

Over the history of additive manufacturing development, several different techniques have been developed. These technologies can be differentiated using the state of the material used: powder, liquid or solid.
Powder based technologies can be subdivided into ones that use just a single component powder and ones that use powders that contain the base component plus a binding material. Of the powder-based technologies there are: selective laser sintering, selective laser melting, electron beam melting, laser deposition and 3D printing. 3D printing is the only technology of these that require the use of a binder.

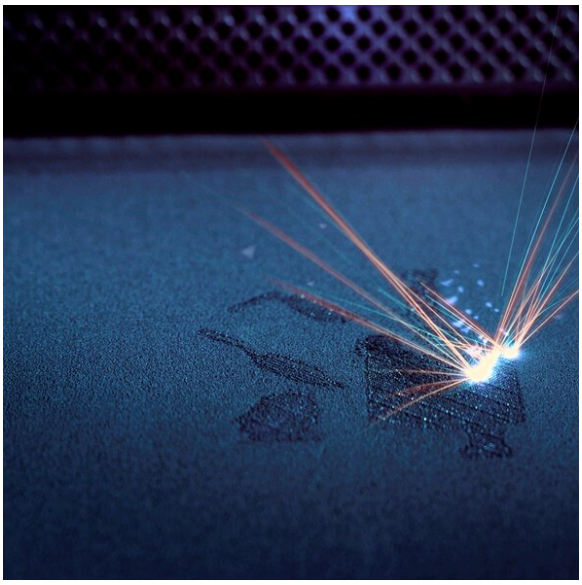

*Figure 3.1: laser beam in powder bed fusion machine*

Selective laser sintering (SLS) and selective laser melting (SLM) is a technology based on the solidification of a powder bed, layer by layer. The energy source used to solidify the powder is a laser, usually a ND-YAG type. The laser itself is fixed and its beam is deviated to the desired position thanks to a set of actuated mirrors and lenses. After the first layer is built, the build platform on which the piece lays, lowers by the thickness of the layer and a new layer of powder is distributed on the surface. The powder is levelled with the aid of a roller or wiper in order to avoid irregularities on the piece. The excessive powder goes into containers specifically for overflow. The process of solidification and distribution of the powder is repeated until all the layers are built.
The differentiation between SLS and SLM denotes the material that is being used. In the case of metal, the technology is called SLM; for plastic, SLS. Historically, SLS machines also used metal powder. Before the 2000s, the metal powder contained bronze particles which would melt before the rest of the powder, bonding everything together and forming a sintered part.

After technologies were developed to melt and fuse the base metal, the technology name was changed to more accurately describe the process.
Once a metal part is created, it needs to be put in an annealing oven in order to remove the stresses caused by shrinkage. Shrinkage is a phenomenon that is caused by the change in density when the powder is melted into a liquid and then cooled into a solid. In order to prevent physical deformation from the shrinkage, support structures are printed. The supports are also used to anchor the first layer to the base.
The materials used with SLM for metal are AlSi10Mg aluminum alloy, biomedical cobalt and chromium, motorsport and aerospace cobalt and chromium, stainless steel, moulding steel, Inconel IN625, Inconel 718, titanium alloy Ti6Al4V, and gold alloys.
In the case of creating polymer components through, there is no need for supports; thanks to the highly compact powder, shrinkage is negligible. Shrinkage can, however, become a concern when there are large temperature gradients within the structure. This is resolved by pre-heating the print chamber at temperatures close to the melting point of the material.
SLS for polymers is the only technique which allows 3 dimensional nesting. Nesting consists of the saturation of the build volume by stacking different parts on top or next to each other. This is possible because the non-sintered plastic powder acts as a support to the new components and allows them to “float” in the print volume.
The materials used for SLS for plastic can be production-quality thermoplastics. Among these are Duraform (a Nylon 12), Castform (polystyrene for foundry) and PEEK, all produced by 3D system.

Electron beam melting (EBM) uses a similar principle. The difference between EBM and SLM can be found in the source of energy: while the SLM uses laser, EBM uses an electron beam to melt the metal powder layer. The electron beam is generated by warming up a tungsten filament to temperatures higher than 2500°C. It is necessary to create a vacuum in the printing chamber in order to avoid a possible deviation of the electron beam caused by air molecules. The beam is controlled by a set of electromagnetic lenses which deviate the beam to the desired spot, thus, the only movement of the platform is along the z axis. The powder bed is preheated to reduce shrinkage.
The quality of the fusion is very high due to the vacuum created in the chamber. The metal density obtained with this technology is very high relative to other methods.
The only producer is Arcam, a subsidiary of General Electric, who offers four different machines.
The materials processed are biomedical grade cobalt and chromium, aerospace and motorsport grade cobalt and chromium, and titanium alloys.
EBM main applications are aerospace components, biomedical prostheses, and turbine blades.

Laser deposition is based on a different building strategy. There is no powder bed, instead, the metal powder is directly deposited on the desired location. The nozzles that deposit the powder are mounted laterally with the laser on the same robotic arm. The technology started as a part repair method but has developed to being possible to also make whole parts. The advantage, compared to SLM, is their high build volume, up to a cubic meter. Moreover, thanks to the presence of two nozzles, it is possible to create alloys or multi-material components in the machine. On the other hand, the freedom of creating complex shapes is limited because the nozzles must physically move to each point where material is needed. The producers of these types of machines are Optomec, DGM More Seiki, DMD 3D and Prima

Industrie. The materials compatible with the technology are stainless steel, nickel alloys, copper and brass alloys, chromium coral molybdenum alloys, weldable steel and stellite alloy.

The last technology based on the use of powder is “3D printing”. It involves the bonding, layer by layer, of select locations on a powder bed. The powder does not melt but is held together with the use of a binder. The binder is deposited on the desired spot in the form of small droplets, which diffuse within the powder and “glues” the particles together. The process thus, does not involve high temperatures in the first phase. If the powder is metallic, the part requires subsequent sintering and infiltration of the binder in order to replace it with the desired material, usually bronze. In the case of polymers, there is still need for binder infiltration and replacement to improve the performance. The sequence to build a layer is: deposition of a layer of powder, selective deposition of the binder, solidification of the binder through infrared (IR) light.
3D printing is primarily used for functional prototypes and patterns for moulds.
3D printing can print using both metals and polymers. In the case of polymers, polymethylmethacrylate with a sand substrate is used. The metals that are available are stainless steel, Inconel alloys and iron.

Let’s now look at the technologies which use a solid material as its input. The only two existing technologies that exist in this subgroup are fused deposition modelling and electron beam additive manufacturing.

Electron beam additive manufacturing (EBAM) is a technology based on the fusion of a metal wire. The fusion is made possible thanks to an electron beam source. The melted metal wire is deposited on the required spots forming the layers. The platform is usually steady with the nozzle and energy source fixed to a mechanism that can move in all three axes.
Like EBM, the work chamber requires a vacuum in order to function. A big advantage to this method is that there are potentially no limits for the build volume, although creating and keeping vacuum in an increasingly large chamber is a very complex challenge.
The materials available for EBAM are titanium, titanium alloys, tungsten, tantalum, niobium, stainless steel, and copper-nickel alloys. It can be noted how all the materials listed are weldable. This technology is still in its development phase.

The other technology that uses solid material is fused deposition modelling (FDM).
This process is based on the extrusion of a filament onto a platform in order to build the layers. The materials used for the filament must be thermoplastics. This is because the filament is warmed up to a certain temperature (depending on the material) so that it can be extruded and bonded onto the platform or existing layers. If the temperature is too aggressive the filament will become too fluid and there is a risk that the tolerances will not be respected. Previously, early development machines only contained a single extrusion nozzle. However, after years of development it is standard that professional machines have two nozzles. One of the nozzles deposits the material for the part, the other one deposits the supports material. One of the advantages of this technique is that the support structure can be printed using a sodium hydroxide soluble material.
The materials used with FDM are: Nylon, ULTEM, ABS, polycarbonate, and PPSF.
With this technology it is possible to create production quality parts.

A similar technology which could be considered an evolution of FDM is Continuous filament fabrication (CFF). The technology was developed by the American company Markforged. CFF

has the same process as FDM but with the advantage of having an additional nozzle. This nozzle is used to deposit another filament with better mechanical properties. The reinforcement filament is integrated with the standard material matrix, bringing higher performance qualities to the component. The materials used as reinforcement are Kevlar, glass fibres, and carbon fibres. Relative to parts made with standard FDM machines, CFF can increase the stiffness along the z axis. Markforged, with this machine line, also implemented a control system which monitors the part while its being made and ensures that the tolerances are being respected.

There are two methods that use liquid as their base material: inkjet printing and photopolymerisation. The latter is further divided into two subcategories that differentiate the photopolymer activation method between laser and UV lamp.

Drop on demand is the technology that uses the method of inkjet printing. In principal, it works by depositing a low melting point thermoplastic material, milling the deposited surface flat, lowering the print platform, and repeating the process. The milling step is needed due to the irregular geometry created by the partially melted material. This phase is beneficial because it allows adaptive slicing, which is the ability to have differing thicknesses for each of the layers. Adaptive slicing is very hard to achieve using other methods of AM. The material is “loaded” into the machine as granules which are warmed up to their melting point when deposited. The consistency of the material are similar to that of wax. There are two different nozzles: one for part and one for supports.
This technology, formerly used in dental and medical industries, is now commonly used for lost wax casting for jewellery.

Stereolithography is the photopolymerisation technology that uses laser as its activation energy source. As previously mentioned, it was the first additive manufacturing technology to be developed and patented. It consists of a tank filled with a liquid photopolymer, also called a resin, which gets selectively solidified with the energy emitted by a laser. The platform lowers and a new layer can be treated. Like other laser based technologies, the laser is mounted rigidly, and the beam is deviated by actuating mirrors. The laser does not solidify the whole surface of the exposed layer. Rather, it builds the external surface together with lines that partially connect the perimeter, trapping most of the uncured resin inside. The resin is then solidified after the shape is completed in an oven with UV lamps.
This technique is only used for prototypes because the resin is not recyclable. Part and supports are made with the same material but the supports can be printed with a much lower density. The supports are removed and disposed of after printing. The supports are not required to physically support the overhanging parts, but to avoid shrinkage. Shrinkage is caused by the change in properties between the liquid and solid state. Stereolithography machines must be used in a controlled environment with specific temperature and humidity values in order to print properly and for safety reasons. The resins used also need specific requirements.
Stereolithography is used for high precision functional prototypes and for the “QuickCast” method. QuickCast is the process of printing an object with an internal honeycomb structure. This part is then used to create a ceramic shell for metal casting.

The photopolymerisation techniques that use UV rays as the catalyst for solidification are known by two commercial products with the names Polijet and Project. The process for both of these technologies are more or less the same. First a photopolymer is deposited onto the

surface and is then immediately solidified via UV lamps. The machine has an arm that is suspended over the entire length of the work area. This arm is covered by many nozzles along the y direction that are individually actuated. This arm can move along the x direction while depositing the resin from the necessary nozzles. Along the length of this arm, there are two UV lamps, one on either side of the nozzles. These lamps are actuated depending on the direction that the arm is moving. Some of the nozzles are used for the supports and deposit a different material which can be dissolved in water or other solvents. The photopolymers are sold in cartridges, which is beneficial because there is no need to take precautions while handle the material. Another benefit is the ability of manufacturing digital materials by combining different materials during the production process. These machines are only used for prototype creation and models for silicon replication.

Another photopolymerisation method exists that uses UV rays directed through light projection. Mainly used in the jewellery industry due to the small build volumes, it uses a projector to solidify the whole photopolymer layer at once. The lack of a single laser point makes the process faster than the other techniques. The supports must be made of the same material as the part. Most of these machines have the projector installed at the bottom of the tank. The projection passes through a UV transparent wall and solidifies the bottommost layer. This way allows the piece to grow upward. Nevertheless, there are some machines that work by solidifying the top layer and lower the platform.


*Figure 3.2: additive manufacturing products*

As hinted at throughout this chapter, there are many advantages to additive manufacturing technologies. A major advantage, that leads to other consequential advantages, is the freedom of manufacturing virtually any type of geometry, resulting in nearly unlimited design freedom. Previously, some mechanical and thermal qualities of components had constraints related to the restrictions of traditional manufacturing techniques. In some cases, complex geometries could be created using complex machines like multi-axis CNC mills, but this method, in most cases, is more costly, time consuming, and skill intensive when compared to AM machines.
With this added freedom of design provided by AM techniques it is possible to create lighter components, stiffer components, components with better thermal characteristics, integrated parts with reduced joints, and potentially components with benefits not yet realised.
Another major advantage provided by AM technologies is the time that it takes to make changes to a component. When a change is needed, the CAD file just needs to be modified

and sent to the AM machine where it will quickly (relative to other methods) produce the new part. The same principle allows high customisation of a part for a client.
For some companies, the main advantage may come as a cost reduction. Although AM machines are themselves expensive, the cost of the machinery that they replace may greatly exceed the investment for AM technologies. The cost of labor is another advantageous consideration. Unlike traditional subtractive manufacturing methods, most AM machines do not require the attention of highly trained personnel. Several machines can be ran simultaneously with little oversight. When compared to something like a CNC mill, where a highly skilled machinist must first prepare the g-code and then monitor the process of the manufacturing, AM is clearly a better choice.
There are also environmental advantages that result in cost savings for a manufacturer as well. The amount of material wasted in AM is very small when compared to subtractive technologies. The average buy-to-fly ratio, the ratio of the initial amount of material used for the production and the amount of material in the final component, is 8:1 for conventional machining, whereas only 1.5:1 for additive manufacturing. This low buy-to-fly ratio reduces the $CO_2$ emissions on several fronts. Firstly, very little energy is wasted shipping the raw material to the manufacturing facility. In the case of traditional manufacturing where the buy-to-fly ratio is 8:1, 7/8 of the mass transported is not even used in the final component. Furthermore, there is energy wasted in the recycling of this material waste. In the case of the traditional manufacturing environment, that 7/8 of mass must then be shipped to a recycling centre where even more energy is invested into re-melting the material. In some cases, it may be the situation where a company needs to ship pre-made components. Shipping those individual components does not efficiently take advantage of the packaging space while shipping. If they switch to in house AM, the raw material can be shipped in bulk and as efficiently as possible.

All of these technologies and their benefits find applications in many different fields.
Aerospace companies have been investing in the production of lightweight components and have begun using additive manufacturing technologies to create prototypes. There is a big potential for the reduction in pollution when AM based designs are implemented into aircrafts. The weight of aircrafts has a big influence on their emissions, especially during take-off. When lightweight components are installed in aircrafts, the fuel usage can be reduced by up to 1/3 in the case of short distance flights.
The automotive industry is using the technologies during the development stages of production cars but is also creating lighter components used on cars driven for motorsports.
The biomedical field is one that has been revolutionised by the use of additive manufacturing technologies. It has made it possible to produce trabecular structures for bone replacement surgery. This particular structure helps osseointegration and leads to an easier and faster recovery.
Maxillofacial surgery has been implemented using reverse engineering software and the reproduction of a patient's specific morphology in order to make advanced pre-surgical simulations. This step lowers the chances of unexpected events that may make the surgery more difficult. The ability for AM to create light structures and use light materials reduces the issues previously caused by unnatural, heavy loads placed on the cranium in case of jaw or facial implants.
3D bioprinting is a technology based mostly on inkjet printing (although stereolithography and other technique are occasionally used). This technology produces tissues and even organs that can be implanted in human bodies. Through the combination of biomaterials, cells, nutrients and other activating factors, it is possible to produce body parts, including vascular systems. A sugar or gel matrix is used as base on which layers of cells are deposited.

In Archeology, some additive manufacturing technologies are being used to replace missing parts of antiques and monuments exhibited in museums. They are also using 3D printers to make souvenirs replicating the famous pieces.
Jewellery making is another field that is largely adopting additive manufacturing machines to produce complex and articulated shapes to create modern, unconventional pieces of art.
Even in the food industry additive manufacturing is being used. NASA has investigated the possibility of having a technology that could print food suitable for astronaut's diet requirements in order to reduce food waste. In 2018 a technology was developed by an Italian bioengineer that was able to create a meatless food that mimicked meat's flavour and consistency. The technology is based on the printing of vegetable proteins in order to obtain a meat substitute.
The food industry also uses additive manufacturing techniques to create particularly shaped items using different ingredients such as mashed potatoes, jelly or chocolate powder. The technologies used are based on extrusion, selective laser sintering, binder jetting and inkjet printing.

Despite all the positives of additive manufacturing technologies and the implementations already seen, there are some limitations and challenges for the technology.
The machines were created merely for prototypes and are not provided with automation or control systems. Some machines are beginning to become implemented with on-line feedback control but they still need improvement before they become fully automated.
Another big limitation is the build volume. Most machines do no provide volumes bigger than 400x400x400 mm. This is primarily caused by the challenge presented by needing to maintain a constant temperature, and sometimes pressure, in large volumes.
Depending on the additive manufacturing technology and the subtractive technology it is compared to, the process can be a slow one.
In most cases, the components also need post processing and finishing operations. It is likely that the tolerances and surface roughness of the part do not meet the requirements of the design. Additional post processing may need to be conducted when there is the presence of support structures, which is common.
The materials compatible with the technologies are also much more limited when compared to the ones available for standard technologies. Moreover, the cost of the materials for AM is much higher.
Despite these issues, the additive manufacturing field is developing very quickly towards overcoming the issues just outlined.

# 4. Original Product Overview

The object of this thesis is to conduct a study on the design of an electric scooter.
As outlined in the section “micromobility”, a scooter is a micromobility transportation device that has spread out through most all developed countries in the past few years. There are several major factors explaining the recent growth in popularity for these devices such as their low emission impact, cost, and comfort. A more thorough background behind micromobility and electric scooters can be found the in the above section “micromobility.”

As found in many vehicles, the electric scooter has a steering component made with handlebars.
Like in bicycles, the user holds the handlebars and rotates them to move right and left. The handlebars are connected to the front wheel through a solid cylindrical structure called the stem. The front wheel is connected to the stem via a fork and spring. The spring works as a force distributer and prevents quick and jerky movements to be transmitted through the structure and into the user. A common example of this is when a scooter drives over a bump or step.
The user places his or her feet on a board which is usually made of wood but can be observed to be made of other materials.
The board is fixed, through a set of screws, to the frame. The frame has a component called the “head tube” which connects the frame to the stem. The “head tube” has a set of bearings that allow the rotation of the steering while also taking the forces experienced from the wheel.
In this specific model, the back wheel was decided to be a set of two wheels rather than one in order to increase stability.
In order to implement a dual wheel set up, a clever design solution developed for skateboards was used: a truck. The truck allows the back wheels to have the same rotation angle and keeps them at the same distance between each other while restricting two degrees of freedom.
The components just briefly described are the structural components of the scooter and are what the study of this thesis concerns.
In addition to the previously mentioned components, there is the electric motor, which is positioned in the front wheel, the braking system, the headlight, and the stop lights, as required by the law.

In order to operate the device the user must first activate an on/off switch. Once standing on the scooter the electric motor is activated with the acceleration handle. The motor causes the front wheel to rotate, propelling the rest of the structure forward. When the user has to take a turn, they rotate the handlebar to the desired direction causing the trajectory to change. This drags the frame behind and causes a rotation of the truck and thus the back wheels.

The main load acting on the structure is the weight of the user. For the purpose of the study, the user was assumed to have a mass of 100 kg. The force acting on the footboard is then 981 N. For the sake of safety the force was later rounded up to 1000N.
A limit stress case was included in the calculations and in the development of the problem. In order to design the components to withstand true-to-life conditions, a high force situation was developed.
The situations considered is when the scooter hits a bump or a goes up a step.

For this study's situation, the height of the bump was assumed to be 2 cm, and to have an approximatively spherical shape.
In order to obtain the forces acting on the different components, we first must calculate the direction of the force that is sent from the bump to the wheel and that is then transmitted to the structure.

The direction of the force depends on the height of the bump and on the dimension of the wheel.
It can be calculated graphically by measuring the angle included by the horizontal and the segment that goes from the tip of the higher part of the bump, to the center of the wheel, as illustrated in Fig. 4.1.

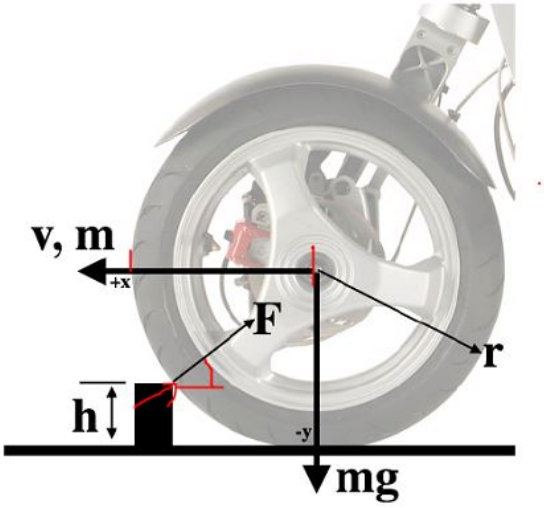


*Figure 4.1: Wheel free body diagram*

However, in order to reach a higher level of accuracy, the angle was calculated through geometrical considerations.
The equation used is the following:

$$\theta = \frac{\pi}{2} - sin^{-1}(\frac{r-h}{r}) \tag{4.1}$$

where θ is the angle between the horizontal line and the segment that connects the top right tip of the bump and the centre of the wheel
r is the radius of the wheel
h is the height of the bump.

The scooter model that was studied has two different sizes of wheels thus two different angles must be considered. This difference In radius and angles yields two different forces for the front and rear wheels.
The front wheel diameter is 25 cm, making the radius 12.5 cm. The rear wheel diameter is 20 cm, its radius is 10 cm.
The height of the bump is 2 cm.

By using the equation the following results are obtained:
Front wheel θ is 32.8°, it will be rounded to 33°.
Rear wheel θ is 36.8°, it will be rounded to 37°.

In order to find the magnitude of the force, the chart shown in Fig. 4.2 was used.

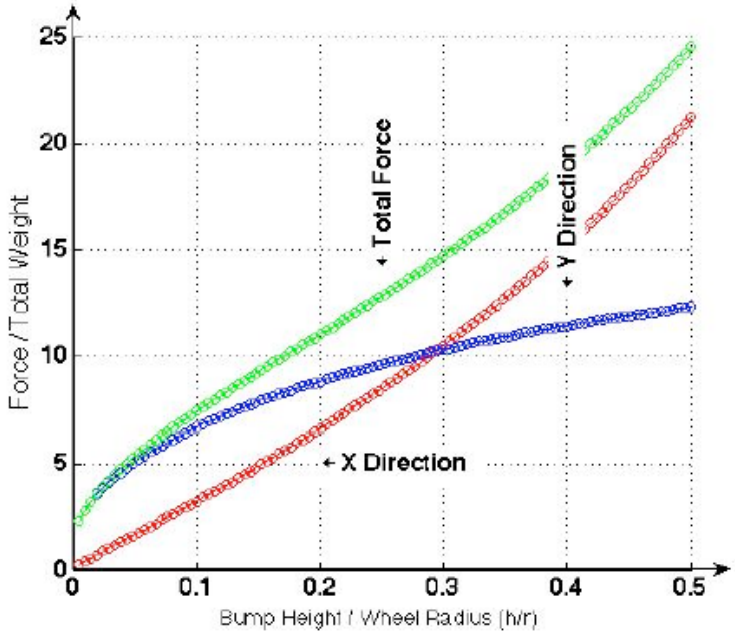


Figure 6: The forces (in g's) on a wheel of radius r in the x and y directions.
Notice how the force in the x-direction approaches infinity as h/r increases.

*Figure 4.2: force chart*

The abscissa of the plot represents the ratio of the height of the bump to the wheel radius (h/r).
On the ordinate the force and total weight ratio is plotted.
The h/r factor for the front wheel is 0.16, for the rear wheel is 0.2.

The remaining data needed to solve for the force is the total weight on each of the two wheels. The user was assumed to distribute its weight at a 6/10 board length from the front wheel. An easy calculation is needed to compute the weight distribution.
The distance between the two wheels is 1 meter. Using this 1m dimension it can be said that in the image 4.3, $l_1$ measures 60 cm and $l_2$ measures 40 cm.

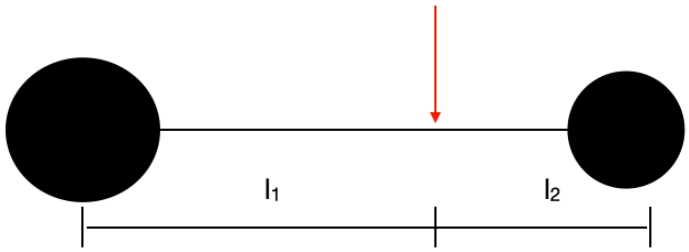


*Figure 4.3: load distribution*

The force on the wheels can be calculated through the following equations:

$$W \times a = R \times L \quad (4.2)$$

$$R + S = W \quad (4.3)$$

Where W corresponds to the weight force, 1000N; a is $l_1$, 60 cm; R is the reaction at the back wheel, L is the total length, thus $l_1$+$l_2$, 1 m.
From the first equation, R is 600 N.
The second equation is used to find the reaction at the front wheel (S), which is 400 N.
Now that the forces and ratios have been found, it is possible to define the bump force through the chart.
From the ratio value on the abscissa, a line is drawn upward until it intersects the green line.
For the front wheel, using a ratio of 0.16, it is found that Force/total weight = 9g, where g is the measurement unit for the force. Thus, for the front wheel, the force is 9x40=360 N. This force will be rounded to 400 N to (be more conservative).
For the rear wheel, with a ratio of 0.2, the value obtained with the intersection of the vertical line and the green line is 11. Force/total weight= 11g, force is then equal to 11x60= 660 N.

In the final product there will be a spring/damper system above the fork. This, ideally will reduce the high loads induced from these impacts by spacing the impact over time and absorbing some of the energy. However, for this study, these effects were neglected. This was because these dynamic situations vary greatly and are affected by the design of the spring/damper system. Additionally, the effects of these systems would be relatively negligible so the structure design was continued without their consideration.

# 5. Design for Additive Manufacturing

In this chapter the development of the main experimental work will be shown and explained.
The aim of this study is to evaluate which components of a scooter could be produced by means of additive manufacturing technologies.
In order to make this evaluation clear, a process of re-design will be made, many aspects will be considered and compared, such as weight, resistance, safety factor, cost and process.
The whole process will be shown for each component.

In this particular case we are talking about design for additive manufacturing. So far, only the functioning and bases of the technologies were explained, but how and why do we use these technologies?

The way a design is approached, and which additive manufacturing technologies are used for a particular product depend greatly on the type of product being produced.
For example: in the biomedical field, personal hearing aids or heart valves are commonly produced by means of AM technologies. Because these types of items need to be personalised for each user, reverse engineering techniques are used to digitally reproduce the environment where the biomedical item will be placed. Observing the case of the hearing aid: The client first gets a scan of his ear which creates a digital model of the inner ear. A hearing aid model is then created with software using the 3D scan of the ear, creating a perfect match. Lastly, the CAD file is sent to the proper AM machine and is then physically manufactured for the patient.

This is not the same design case that was followed for the development of the scooter. In the case of this project the goal is to optimise existing scooter components and take advantage of the possibilities made by AM. Because of the limits that subtractive technologies impose on the current designs there are areas where the material is not needed but still exists.
The benefits that are being sought after by optimising the design are to reduce the components weight, increase their resistance and have a higher weight to stiffness ratio. Thus, the design had the need to start from the original components.

Although not an important consideration for this design, designing for additive manufacturing can be used to achieve different goals. These include, maximising specific mechanical properties, optimising dynamic behaviour and thermal performance, reducing the number of components, and integrating multiple functions into just one element.

For this study, the software used was “Solid Thinking Inspire” developed by the American multinational company “Altair Engineering Inc.”. The outline below follows the steps understood by working with said software, however, the iterative process shown can be assumed to be very similar in all other software used for this purpose.

First, the original “baseline” component is uploaded. The material properties, constraints, load conditions, and other information discussed below are input into the program and the system is evaluated by the software. A modal analysis is computed to ensure that the component will withstand the forces and stresses expected from the use of the product with the required

safety factor. The analysis first studies the static behaviour, then the almost-static behaviour, then the dynamic behaviour.
After this analysis is complete, there are two cases that will be resulted: over the safety factor or under.
In the case of a “failure” the model is automatically modified by adding material to critical, high stress concentration areas. Another modal analysis is computed and the cycle continues until the stresses either match or exceed the set safety factor.
When the software detects that the analysis yielded a “passing” situation it moves into topological optimisation. This is the phase in which the software works towards achieving the user set targets. An example of said target could be a weight reduction amount or a certain frequency response value. In addition to setting these targets, the user also must input the design constraints of the system, for example a hole or an area that will be connected to another element. This is achieved by delimiting the design and non design spaces. The non design space being the part of the model which will not be modified. An example of where this is used is if there were a hole for coupling; there must be enough material around the hole to allow the proper tolerance and the insertion of the other element so the user explicitly tells the software that no material around said volume can be modified.
The software uses the aforementioned restraints and goals to selectively remove or add material each iteration. Nodal analysis is made after each change and if the system enters the “fail” case again material is added to the high stress areas and the cycle repeats. The result in most cases is an organic shaped, lighter component with better mechanical properties for the purpose of the component.
After the software has decided that the optimisation is complete the designer must then ensure that the results are good. If the analysis does not yield satisfying results, the software allows the shape to be thickened by increasing the user set “allowable mass”. The analysis is computed again and this step is repeated until satisfactory results are obtained.
Once the designer reviews and approves the generated design considering the safety factor, displacement, stiffness, frequency etc. the design moves to the following phase: solid model reconstruction.
At least in the case of *Solid Thinking Inspire,* the output file from the iterative design is not a usable solid model. The format of the file made so far is not a solid, instead it is just a nodal finite element model. The software offers a function that reconstructs the shape to a 3D model, even though it is not assimilable to any standard geometric shape such as parallelepipeds or cylinders. The software function is called “PolyNurbs” and works by “wrapping” the FE model shape and creating a solid starting with an oval shaped volume. There are many other sub functions that can be used while going through this step. An example of this is the bridge function which allows to add material to two or more separated ends by following the shortest path. The result is a smooth and rounded arm (in case of two ends) or branches (in case of more ends).
After the solid model creation is completed, analysis must be computed to verify the desired mechanical characteristics of the model. If all the factors meet the requirements of the design, the model is ready. If the factors do not meet the requirements the model will be modified by re-distributing or adding mass to the proper areas.

Be advised that this was just a brief and general explanation of the process applied in design for additive manufacturing. Many factors can vary depending of the kind of component analysed, and what the goals of the optimisation are. Of course reducing the weight of a high load component has different considerations from changing the thermal or vibrational characteristics of another object.

The following pages now will focus on the design for additive manufacturing applied to the components of an electric scooter.

# 5.1 Steering

The first element of the scooter that was studied is the steering.
The most common and most simple kind of steering arrangement for a scooter is a perpendicular bar that intersects the main steering pipe frame called the “stem.” Both of the pipes are usually made of the same metal, also usually aluminum. The horizontal bar that is gripped by the user is called the “handlebar” and on each of the ends of the handle bar there are the handles. The handles are usually made with a polymeric material which feels softer and nicer at the touch and adds more friction to the grip.
Sometimes this part of the vehicle features a cover box used to store the electronic parts that connect the motor to the acceleration actuator. The electronic box may also be used to hide the wires that connect the breaks on the wheel to the break actuator. The system may vary depending on the type of breaking, if purely mechanical or electric.

*Image 5.1.1: common handlebar*

The original design that needed to be adapted for AM actually had a slightly different connection than the general form discussed above. The handlebar, rather than being directly mounted on top of the stem, was connected through a block joint. A picture of this arrangement can be seen below in figure 5.1.2.

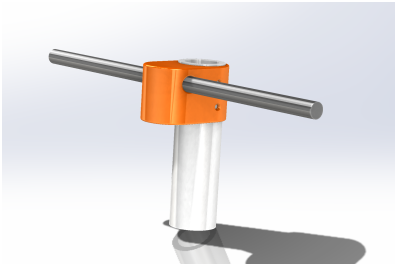

*Image 5.1.2: original product handlebar*

In the following section, the load and force assumptions used in the design of the handle/ steering will be outlined. In the use case of this scooter there is a single user, whose weight is

assumed to be 100 kg. The weight of the user is distributed on the structure through their feet which lay on the platform. The highest stress causing situation was assumed to be the one in which the scooter hits a bump or goes down or up a step. The resultant force caused by the bump acts on the wheels at a certain angle depending on the height of the bump. The magnitude of the force depends on the height of the bump, the weight of the user, and the position of their feet, which was assumed to be at 2/3 of the length of the scooter from the front wheel. As shown in the previous chapter, *product overview*, the angle of the force on the front wheel is 33° from an horizontal plane, the magnitude is equal to 400N.

In this section, the main focus is on the force transmitted to the handlebar from the steering stem. In order to obtain this force, the vertical component of the force acting on the wheel was calculated.
Rather than being completely vertical from the ground plane, the stem is slightly inclined. As shown below in Figure 5.1.3, the angle included by the stem and the direction of the bump force is 163°. This angle is used to calculate the component of the force transmitted to the steering handles through the stem. The magnitude of this force can be found by calculating the cosine of the supplementary angle (180°-163°), and multiplying it by the magnitude of the original force: 400 x cos(17°) = 0.95 x 400 = 383 N.

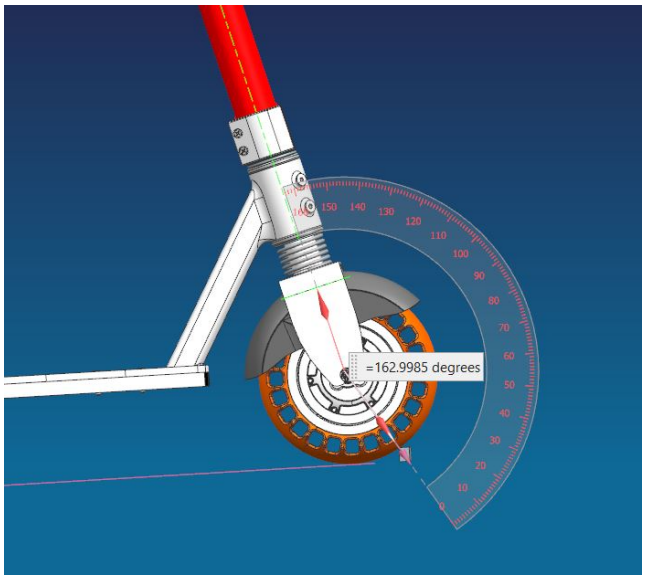


*Figure 5.1.3: bump angle*

The assumption that all of the forces from a bump collision are directed straight to the handle and not distributed to other components may seem like an extreme one and this is intentionally so. There are scenarios other than driving over a bump or ledge that may occur that will impart a high load to the steering section. It is unreasonable to undergo complex dynamic analysis of different scenarios, especially for the scope of this study. Therefore, the worst-case load scenario shown above was selected as an adequate basis of design.

The material of the original component is 6061 Aluminum Alloy. 6061 Aluminum is aluminum alloyed primarily with magnesium and silicon and which is precipitation hardened. The alloy provides good mechanical properties such as toughness, weldability, and excellent corrosion

resistance. It is found in almost all engineering applications and fields as a general-purpose alloy.
The 6061 aluminum alloy's physical and mechanical properties are shown in table 5.1.1.

*Table 5.1.1 - 6061 aluminum alloy's properties*

| ρ (kg/s) | E (GPa) | $\sigma$ (MPa) | $\epsilon$ | $\nu$ |
|---|---|---|---|---|
| 2.70 | 68.9 | 124-290 | 12-25% | 0.33 |

The result of the static analysis of the original component is shown below in Figure 5.1.4. It can be observed that the safety factor's value is higher than 6 in all the areas of the component.

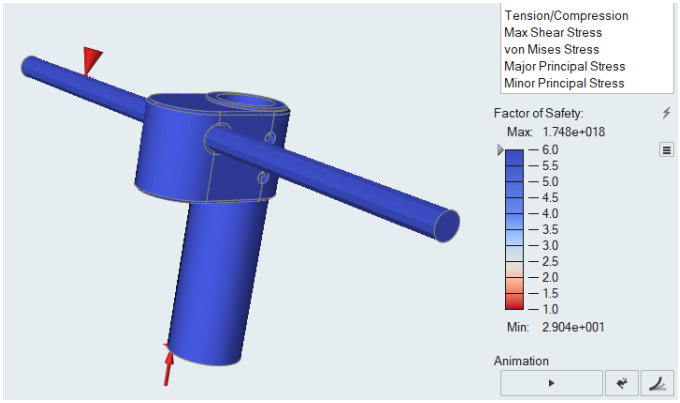


*Figure 5.1.4: original handlebar stress analysis*

## 5.1.1 Component preparation

In order to begin the optimisation process, the component needed to be prepared. The component was uploaded to the software, however, before the analysis was made any accessories or non structural aspects of the original design were removed.
The original component was used as the starting point for this process. The design space was selected to be a 25 cm x 23 cm x 19 cm (base, height, depth) rectangle enveloping the entire existing system and is shown in Figure 5.1.5. The grey box denotes the design space, whereas the blue bodies are in the non-design space. It can be seen that only a small portion of the stem (3 mm) and handles (114 mm) kept their original shape.

As a design note it is important to be aware that at the beginning of the design process, one of the aims of the design was the integration of the handle bar to the stem, to obtain just one piece. We are going to see in the following pages how this is very challenging and economically not convenient at all: it would cost too much money to the producer since the

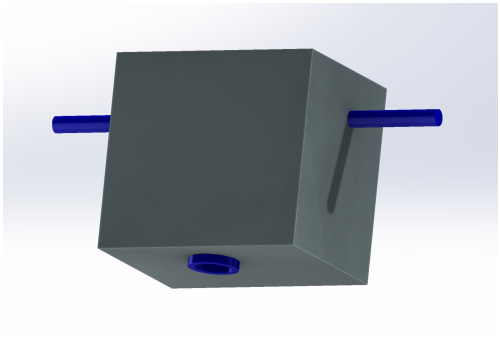

*Figure 5.1.5: handlebar design and non design spaces*

stem is a very cheap component produced through extrusion, whereas it is quite expensive and worthless to produce a long pipe with additive manufacturing technologies. Nevertheless the aim of the design was the reduction of mass and the integration of the handlebar with part of the stem.

It was decided to build the volume slightly above the level of the handle bar in order to give the software more freedom in its design and shape selection. Likewise, the design space allowed the software to modify 20 cm below the handlebars. This was determined primarily as an aesthetic decision, however, cost and manufacturability difficulty would have increased as the design space expanded downwards and with little improvement. The non-design space was selected as the couple that attached to the stem, and the two handlebars.
The component was subjected to a force parallel to the stem. This force was decided to be rounded up to 400 N out of fear of higher than expected load cases. Constraints were applied to the handlebars where the user would resist the force. After the system was defined and set up, the optimisation stage began.

After a few iterations of optimisation and experimenting using the different settings (safety factor, maximise stiffness, mass target reduction) the shape of the steering began to reach a form that was satisfactory and strong enough. Before concluding the design, however, it was decided to create a component that was partially hollow. This change would allow the electronic wires to pass from the handles through the stem without being seen externally. These holes were manually added by importing the Parasolid from Inspire to a CAD software (NX). The solid files were then hollowed as desired and re-uploaded to Inspire for the analysis.

The software created a similar shape as the previous iterations, but some areas, close to the stem, were not able have enough material to allow the machine to create a thick enough and safe wall. Because of this, the idea of englobing the wire holes was abandoned. It will be evaluated after whether or not it is the case of including the holes in a final design.

### 5.1.2 Material selection

As in most of all design considerations, the material selection is one of the most important steps and must be made before the optimisation is started. The proper choice of the material is extremely important because a good compromise of the mechanical properties (overall strength, elasticity, density, thermal properties etc.) will lead to the best solution; in this case in terms of shape, strength, and weight.
Let us consider the original component material. As shown previously, the material was a 6061 Aluminum alloy. Among the metallic materials, it exhibits one of the lowest densities.
It is a relatively cheap material if compared to titanium specialty alloys or other highly engineered materials, and despite its price, provides a competitive strength to density ratio. Other important characteristics of aluminum are its durability and infinite recyclability.

When, as in this case, a design is being considered for additive manufacturing technologies, the choice of the material is more limited. Compared to the materials used in traditional manufacturing methods like subtractive manufacturing, casting, rolling, etc. the number of available metals and alloys is much smaller, and cost becomes a much more important consideration.
The limited amount of materials available for additive manufacturing depends on the fact that they have to be handled and manufactured in a different way. Most of the technologies available for metallic additive manufacturing use a metallic powder. This powder usually is produced through gas atomisation.
Gas atomisation is a generic definition for more specific processes. Among the most common gas atomisation methods are air atomisation, inert gas atomisation and vacuum inert gas atomisation. In general, the process involves on injecting a high pressure gas onto a stream of molten metal flowing through a small opening. The gas breaks the metal into fine powder.
Some other AM technologies involve the fusion of a metallic wire. In that case, the production of the metallic material surely is different and most likely simpler to produce; however, the AM machines that use this technology are not as common as the ones that use metallic powder. Moreover, the cost of the machine is higher, so in this particular case, the overall expense would end up being higher.
Before making a material selection, first the material requirements needed to be understood and listed. Primarily, considering the use case of an easy to transport scooter, it is obvious that weight plays a very important role. Thus, the density of the material has to be low enough to satisfy certain weight requirements. It needs to be resistant to corrosion and more generally to any kind of weathering because it will be used outdoors. Another limit imposed on the choice of material is the cost; the scooter is not meant to be an extreme luxury item, but more of a high quality yet reasonably affordable one.

Because the handlebar does not undergo high forces, the focus for this component falls on weight reduction with no need to look for highly technical materials that present impressive mechanical properties. Based on these considerations, the choice narrows towards aluminium alloys.
Heavier materials such as steel were not considered for this component because of their higher density (around 7.75 g/cm$^3$ steel vs. 2.7 g/cm$^3$ aluminum) which would make the part's weight higher than desired. Titanium alloys have a low density relative to their great mechanical properties but its cost is way too high for the budget of this particular part.

Looking back at aluminium alloys, the only ones that are available for additive manufacturing are listed here: AlSi10Mg, AlSi7Mg0.6, AlF357 and Scalmalloy.

Shown below is the table 5.1.2 with the properties of the listed aluminium alloys.

*Table 5.1.2 - aluminum alloy properties*

| | $\rho$ (g/cm$^3$) | E (GPa) | $\sigma_{ts}$ (MPa)* | $\sigma_{ys}$ (MPa)** | $\epsilon$ (%) |
|---|---|---|---|---|---|
| AlSi10Mg | 2.65 | 70 | 300 | 190 | 2 |
| AlSi7Mg0.6 | 2.67 | 70 | 400 | 240 | 8 |
| AlF357 | 2.67 | - | 340 | 265 | 11.5 |
| Scalmalloy | 2.67 | 65 | 490 | 450 | 8 |

The latter two materials shown in the table are attractive for their higher mechanical properties, but, like titanium, it was decided to not use them because of their higher price.
The cost of AlSi7Mg0.6 is slightly higher than AlSi10Mg and, even though AlSi7Mg0.6 has better mechanical properties, AlSi10Mg was chosen as the best metal to use because of its better availability from the Italian additive manufacturing suppliers and for its lower cost.

As shown above, only metallic materials were taken into consideration. However, it seemed prudent to also evaluate the behaviour of the component using polymeric materials as well. These, like the metallic materials, must also be compatible with additive manufacturing machines. Fortunately, there is much higher availability for these materials compared to metals.
An interesting group of polymers are polyamides (PA12, PA6). They exhibit good mechanical properties and have high chemical and abrasion resistance.
Nylon (polyamides) and most other polymers alone would not match the characteristics required by the component, but some technologies allow the combination of this materials with glass, carbon or kevlar fibres, which improve the overall behaviour/properties.
Another material that was considered is one which is called PEEK (Polyetheretherketone), a so-called “techno polymer”. It is widely used in aerospace, and presents a higher level of mechanical properties than many other polymers. It is the only polymer which melts around 343°C.
The Nylon family material’s properties may vary by big amounts depending on the AM technology they are being used with. For example if they are used in FDM (fusion deposition modelling) their properties will vary depending on the direction (x,y or z), and will typically not have good mechanical behaviour along one of the 3 axes. In the case of a Nylon being used with a SLS (Selective Laser Sintering) technology there are many factors that can influence the mechanical properties. The most important factors that can make these changes are: the temperature in which the polymers are subjected, the temperature gradient, and the time in which they see the change in temperature.

---

* *$\sigma_{ts}$ stands for ultimate tensile strength*

** *$\sigma_{ys}$ stands for yield strength*

The initial materials analysed were CarbonMide and PEEK (produced by the company EOS), kevlar-reinforced onyx and carbon fibre reinforced onyx (sold by the company MarkForged), Carbonpeek, Carbon PA and PEEK (produced by the company Roboze).
Their properties are shown in table 5.1.3.

*Table 5.1.3 - selected polymers' properties*

| | $\rho$ (g/cm$^3$) | E (GPa) | $\sigma_{ts}$ (MPa) | $\sigma_{ys}$ (MPa)*** | $\epsilon$ (%) |
|---|---|---|---|---|---|
| CarbonMide | 1.04 | 6.1 | 72 | - | 4.1 |
| Peek (EOS) | 1.31 | 4.25 | 90 | - | 2.8 |
| Kevlar onyx* | 1.2 | 4.37 | 164 | - | 4.98 |
| Carbon onyx** | 1.2 | 7.73 | 216 | - | 4.22 |
| Peek (Roboze) | 1.30 | 3.3 | 87 | 120 | 3.7 |
| Carbon PA | 1.40 | 15 | 137 | 100 | 1.65 |
| Carbonpeek | 1.36 | 14 | 115 | - | - |

Let us start with the Roboze materials. Their PEEK material has the material properties provided by any PEEK. The "carbon PEEK" is an evolution of Peek where the addition of carbon fibre improves the mechanical properties and makes the HDT (heat distortion temperature) higher. Carbon PA is a polyamide base with a 20% addition of carbon fibre. Of all the above listed materials, Carbon PA has the highest tension modulus and is ideal for performance mechanical applications. All three of these materials are available for extrusion technology-based AM machines. Although they are very interesting materials from many aspects, the have a large drawback which is that they are only compatible with Roboze machines. This has the potential to greatly limit a design if the machines are not diffused among the manufacturing market in which they are being produced, which is likely the case in Italy.

The primary difference between EOS's and Roboze's product line is that the EOS's materials are made for polymer SLS machines. Their PEEK material is what one can expect, a PEEK plastic that is compatible with SLS technology. CarbonMide is a carbon fibre filled polyamide 12 polymer and has excellent stiffness. Unfortunately, however, a similar situation is present with the EOS material line. They present high performance mechanical properties, but because of their high cost and availability issues related to their machines, they were not chosen for this component.

A different availability situation is seen with the Markforged materials. Markforged is an American additive manufacturing company that develops 3D printers, materials and software.

---

** The values reported correspond to the ones of a 10% kevlar reinforced onyx matrix*
*** The values reported correspond to the ones of a 10% CF reinforced onyx matrix*
**** The values are not reported when failure occurs before yielding*

Their machines are well dispersed throughout the industry thanks, in part, to their competitive pricing. Depending on the company needs it may be more convenient to have one of their machines rather than paying a supplier. This is the case we are assuming for this study: the company already owns a Markforged printer and only the cost of the material will be considered.
The Markforged machines that were designed to print the selected materials use “continuous filament fabrication” as its technology. This is a term coined by Markforged and describes a multi-head filament extrusion technology. Onyx is the commercial name for an enhanced polyamide sold by Markforged. As already anticipated, it can be combined with glass, kevlar or carbon fibre filaments. The amount of reinforcement filament can be selected in the design phase but cannot go above 20%.
The price of the carbon fibre filament is much higher than the kevlar reinforced one ($150 rather than $100 for 50 cc). Thus, Kevlar reinforced onyx seemed to be the most reasonable one.
It was decided to research more in order to find lighter and less pretentious polymers.
In order not to exclude other manufacturing technologies and ensure the best solution was found, a few more polymers were investigated: PA6GB40, a glass fibre reinforced Nylon 6, sold for SLS machines; Carbon infused PA12 by Stratasys for FDM; CRP Windform for SLS (later excluded because too expensive); Duraform GF and HTS produced by 3Dsystem, for SLS.

*Table 5.1.4 - Second selection polymers’ properties*

| | $\rho$ (g/cm$^3$) | E (GPa) | $\sigma_{ts}$ (MPa) | $\sigma_{ys}$ (MPa) | $\epsilon$ (%) |
|---|---|---|---|---|---|
| PA6GB40 | 1.04 | 3.8 | 56 | 96 | 1.6 |
| PA12CF* | 1.15 | 7.6 | 76 | 63 | 1.9 |
| XT2.0 WF | 1.09 | 8.9 | 83.8 | 133 | 3.8 |
| ProX GF | 1.33 | 3.7 | 45 | 60 | 2.8 |
| HTS | 1.2 | 5.5 | 48 | 83 | 4.5 |

The optimisation of the steering was carried out for all of the materials that seemed optimal based off of all the considerations I mentioned above. The results of the analysis using many of the materials were showing safety factors far above the necessary value. Because of this it was decided to use an even simpler and relatively weaker material. Analysing the steering with the Markforged material reinforced with glass fibre, kevlar, or carbon fibre filaments improved the performance but unnecessarily so. So it was decided to use the Onyx without addition of reinforcement filaments.
Onyx’s properties are shown in table 5.1.5.

*Table 5.1.5 - Onyx properties*

| ρ (kg/s) | E (GPa) | $\sigma_{ts}$ (MPa) | $\sigma_{ys}$ (MPa) | $\epsilon$ (%) |
|---|---|---|---|---|
| 1.2 | 1.4 | 30 | 36 | 58 |

** The values reported correspond to the properties along the xy plane. The properties along the z axis result in smaller values*

### 5.1.3 Topological optimisation

Once the materials were chosen, the study could go on to focusing on the main study: the actual topological optimisation.
This stage took place mainly on the software “Inspire”.
As mentioned in the chapter “component preparation”, the parasolid file created in NX was imported into Inspire. The materials and their properties were uploaded, and the forces and constraints were applied to the component.

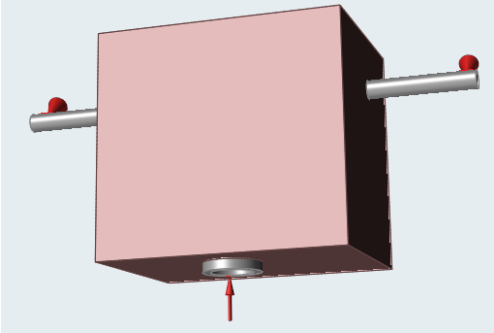

*Figure 5.1.6: steering forces and constraints*

As shown in Fig. 5.1.6, the constraints and forces were applied to the system. The constraints were placed on the handlebar. The force was applied on the portion of the stem that was determined to remain unchanged. The magnitude of the force applied was 400 N.

The first material that was selected for optimisation was the AlSi10Mg. Because this is the strongest material, the first optimisation would provide a good understanding of the material strength needs and the design would be able to be adjusted from that point.
As briefly discussed previously, the software offers different settings for many kinds of optimisations. To begin the optimisation process, the “maximise stiffness” optimisation was selected. When selecting this optimisation option the user is prompted to enter the “maximum allowable mass”. As a starting point, the mass of the original “T” shaped handlebar was input. As a bare minimum the design needed to at least match the weight performance of the original design.

After the software output the first design suggestion, the shape was built into a solid model using the “PolyNurbs” tool and was input into the FEM static analysis software. Using the same loading and constraint conditions as in the optimisation, it was shown that the optimised part had a very high safety factor. This was not a surprise considering the maximum allowable mass was relatively high. This process was iterated a few times, continuously lowering the maximum mass.

For the sake of this study and to understand if a result could be achieved more quickly and without as many manual iterations, the use of the “minimise mass” function was studied. The user input for this function is the minimum safety factor. Using this function the software

should iterate, moving or removing mass until the minimum safety factor has been reached. For this optimisation a safety factor of 1.5 was selected.

Using the design space as shown in Figure 5.1.6 the optimisation took a very long time to run: 10 hours on two occasions. After these first attempts, the design space was edited in a way that would reduce the volume. This would limit the amount of possibilities that the software had to consider and, in theory, would optimise it more easily. It was decided to modify the design space by slightly reducing its depth and by creating a “v” shaped box. The “v” form limits the design space around the stem, this was thought to be acceptable after considering previous optimisations and understanding that the software did not use that space.

Once the design space had been modified, the same optimisation as described above was run. The software yielded a shape very similar to the one obtained by the first “maximise stiffness” optimisations. The only major differences in this optimisation method was a reduction in the thickness of the arms.

The same procedure, using both the “maximise stiffness” and “minimise mass” functions, was done with the polymer materials. These optimisations were computed with the following materials: PA6GB40, Windform XT2.0, and Onyx. The former two were analysed first but consistently yielded unnecessarily high safety factors. After this discovery Onyx was then optimised and yielded satisfactory results.

## 5.1.4 Final design

The last part of the design process for this component consisted of some adjustment to adapt the component to the overall design.
Once the final shape was created and the analysis showed the results that were expected, the file was exported from Inspire, in order to be edited on NX.
The first edits involved modifying the transition between the main arms to the handlebars. The “jointing” surface was rounded in order to appear smooth and to avoid notches. The most significant modification involved creating a constant 7mm diameter hole from the handlebars to the stem attachment point. Adding this feature was to allow the passage of cables from the handles to the stem. Naturally, this step led to changes in the thickness of the component’s arms and required further analysis. The analysis revealed that the walls near the stem were too thin to handle the forces. The area of concern was manually thickened and the connection between the arms and the stem was rounded.

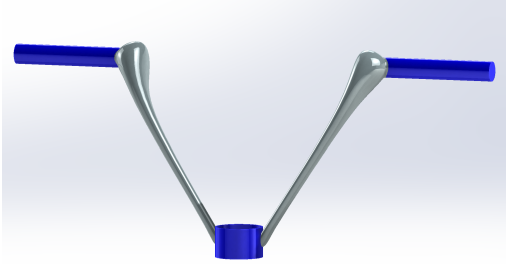

*Figure 5.1.7: final steering design*

Although there may be a technical preference in material for the component, it was decided to include both the metal and the plastic concepts as final designs. This was done in order to allow consideration of the best material to use with cost in mind. The explanation of this consideration can be found in the chapter “Cost analysis”.

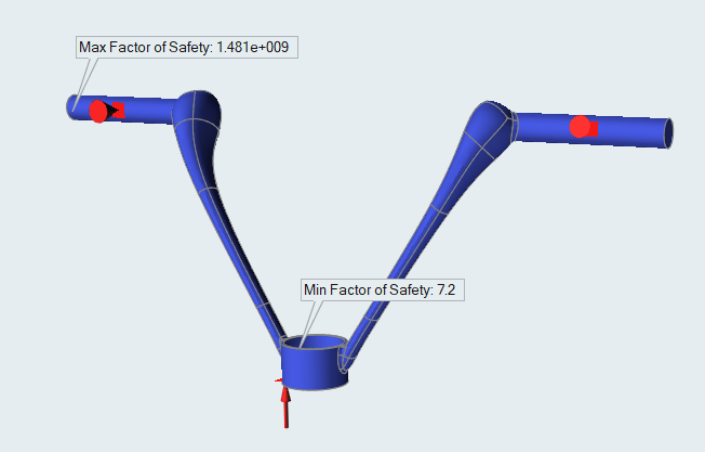


*Figure 5.1.8: steering stress analysis*

The final design using the AlSi10Mg alloy ended up with a mass of 0.516 kg with a minimum safety factor of 7.2.

7.2 as safety factor is considered unnecessarily high. The issue with refining this design by decreasing the wall thickness was a concern with printing issues of such a thin walled arm. The thickness of the walls is of 1.5 mm at the lowest point of the arms.
Despite having an overly strong design it still produced a satisfying result, considering that the original design weight is 1.913 kg. This correlates to a mass reduction of 73% which is what the study was aiming for.

The final design for Onyx has the following characteristics: a mass of 0.232 kg with a minimum safety factor of 2.5. The lowest safety factor corresponds to the area where the arms meet the stem. The mass reduction here is 87%.
The plastic material is preferable mainly because of the low weight achieved. The evaluation of cost can be found in the “cost analysis” chapter.

The decision of dividing part of the stem to allow the integration of the handles with the stem itself does not come without consequences. While we got rid of a joint, another one is still needed.
Three concepts were devised to overcome this problem.
The first solution was to create an engagement through a clip mechanism. It can be seen in Figure 5.1.9-a that the end of the “tabs” there is a triangular wedge which locks the components together once inserted in the proper orientation. The two components will also have grooved features that allow correct installation. This solution can be applied to both the metal and the plastic models.
A second solution is based on a simple hole and thread to allow a screw to keep the two components together.

The third solution, which is only compatible in case that the component is made out of aluminum, is welding.

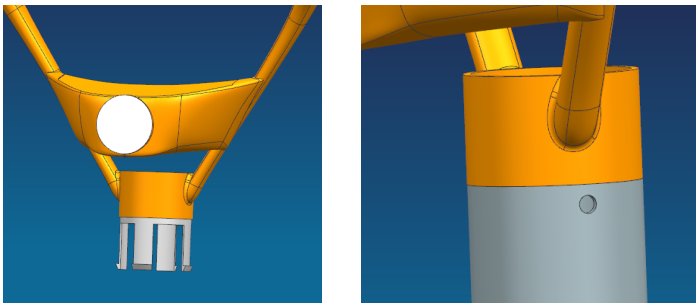

*Figure 5.1.9 : from the left - a) locking mechanism - b) screw mechanism*

## 5.1.5 Process analysis

After the design stage is the verification of the printability of the optimised part. A major part of this stage is to determine the orientation in which the component will be printed, so that the printing process can be simplified.
The printing process depends on which technology is decided to use. Most of the differing printing technologies require printing supports, sometimes to physically support protruding parts, other times, especially when big temperature gradients are involved, to avoid shrinkage and warping.
Netfabb, a software developed by Autodesk, was used to create the supports for each component. It is quite an intuitive process: a parasolid is uploaded on the virtual printing platform, the orientation of the component is chosen and then the supports are generated.
The supports are fundamental but it is important to have as little as possible because they are cut and discarded after the part is printed. Incorrectly designed support design thus leads to a waste of material and machine time. Moreover, the removal of the supports is not easy in most cases, especially with metallic materials, and adds post-processing time.

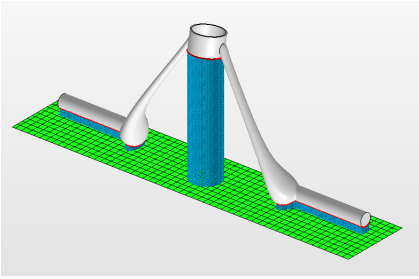

*Figure 5.1.10: orientations and supports suggestion #1*

Netfabb provides a tool called “orient part” which automatically determines the most optimal orientation for the build volume.

Figure 5.1.10 shows the initial orientation determination for the polymer printed component. It can be noticed that, because of the handles, the most convenient orientation still leads to a support volume of 13.93 $cm^3$. More crucially, the plastic model in its entirety would not fit in the machine (Markforged X series) with a build volume of 330x270x200 mm.

Because the design and shape of the steering is limited, designing for reduced support structure was difficult and the final design of the steering did not permit a reasonable volume of supports. Because of this it was decided to get rid of the handles from the printed part and produce them separately. Because they are simply two hollow cylinders, cost savings could also be made by producing them using standard technologies. This decision was made for both the plastic and aluminum designs, both for the same reasons. They will be affixed to the rest of the steering using a clip mechanism or by welding in the case that it is made of aluminum.

Having made this manufacturing decision, the printing arrangement could be made for the aluminum and plastic designs. First, the aluminum layout will be outlined below.

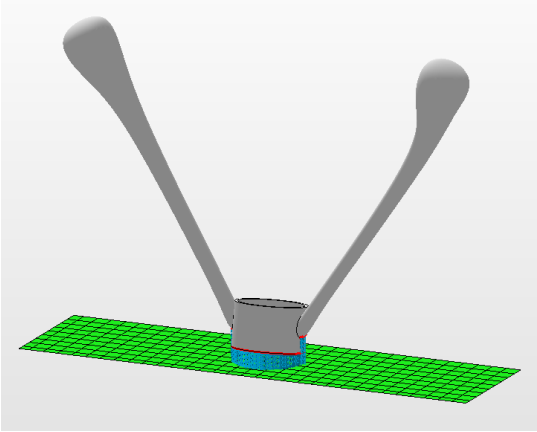

*Figure 5.1.11: orientations and supports suggestion #2*

As shown in the image above, because of the handlebar removal, there is now a much more convenient orientation of the part in terms of supports. This orientation allows the printing to happen with a reduced amount of supports, just 755.89 $mm^3$.
The supports were generated considering a SLM machine, in particular, it was assumed that a EOS M 400 was to be used. This particular machine has a critical angle of 39° and a non critical angle of 42°. The non critical angle represents the inclination of the walls above which there is no need for supports. The critical angle represents the maximum angle below which the supports are absolutely needed. The values included between the critical and non critical angle represent a spectrum in which supports may or not may be needed. The choice falls on the software associated to the machine.
The first layer of the support’s thickness equal to 1 mm and it has a 0.4 mm laser size.
Having more than one parts in the same job is convenient because it is less time consuming; Even though it takes more time to print two components rather than one, the time is saved by

preparing the machine only once. The EOS SLM machine fits 7 parts as shown in Figure 5.1.12.
The volume of the EOS machine is 400x400x400 (mm), so the amount of AlSi10Mg powder needed for the job would be 196 mm (height of the part + 1 mm for the first layer) x 400 mm x 400 mm = 31.360 $dm^3$. The amount of powder in kilogram is 83.1. After being filtered, the excess powder can be reused once the job is done.

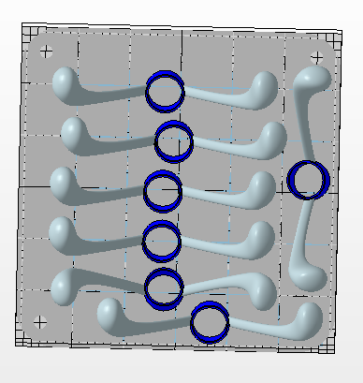

*Figure 5.1.12: arrangement of the steering in EOS M400 (top view)*

If the orientation of the plastic print was kept the same as the metal model, the part would not fit in the Markforged printer because the height of the part is higher than the height of chamber in the machine.
According to the Netfabb software, the most convenient orientation is the one shown in figure 5.1.13:

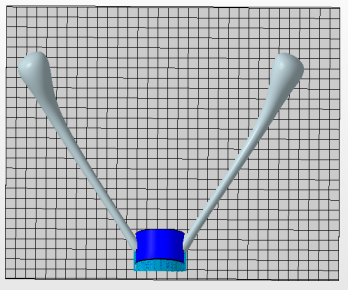

*Figure 5.1.13: arrangement of the steering in the Markforged machine (top view)*

The downside to this orientation is the extended surface of the supports: once these are removed, the part will often need a subsequent treatment to smooth the surface, which means higher post processing costs.

Another solution was then developed to overcome this problem. The arms were to be printed without the portion of the stem, and then connected to the stem through a clip mechanism. This way the support volume is reduced to 0 $mm^3$ (if the first support layer is excluded).

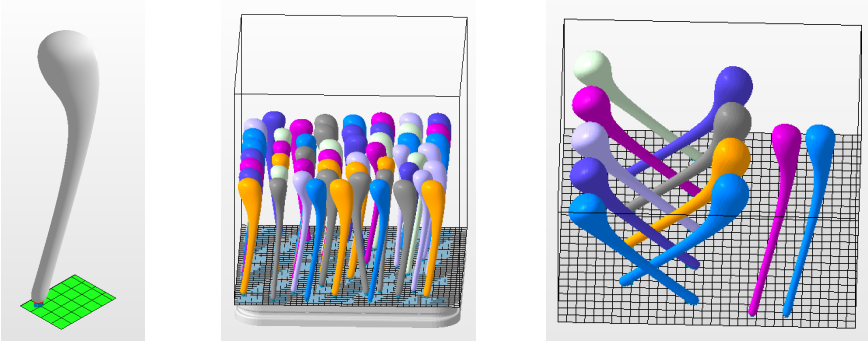

*Figure 5.1.14 a) to the left; b) centre; c) to the right: new arrangements*

In Figure 5.1.14 a) the orientation suggested by Netfabb for the metal component (using the SLM machine) is shown. The picture in the middle (Fig. 5.1.14 b) is the whole platform view configuration of the same machine. 53 parts fit in EOS M 400. The picture at the right (Fig. 5.1. 14 c) shows the configuration of the Markforged machine; the parts result being inclined because the height, as before mentioned, exceeds the height of the machine. Nevertheless, 11 parts fit in the chamber.

# 5.2 Fork

A fork is a mechanical component commonly located in the front wheel of a wheeled device. It consists of two support rods fixed together at the top with a component called a crown. The wheel is supported by its axel which is connected to the end of the two support rods. The load of the wheel is distributed through the rods, converges into the crown. The crown is connected to the steering via the stem. In most cases, the majority of the load is transferred into the frame of the scooter through the “head tube.” Inside the head tube is a set of bearings that transfer the forces from the stem into the frame while also allowing the fork to turn for steering.

Depending on the purpose of the vehicle, the fork may act as a suspension system, when dampers are included. This is mostly used in mountain bikes and in the situations where the vehicle has to deal with rough pavement or rocks. This is not the case for the scooter designed in this study, which is supposed to be used on asphalt in cities.

The dimensions that characterise the fork are the following: offset, width, length, steerer diameter and steerer length.

The material most commonly used to make forks are steel and aluminum for the standard products but when going up in price range forks made out of titanium or carbon fibre can be found.

*Figure 5.2.1: different kinds of forks*

The picture above (Fig. 5.2.1) shows three different kind of forks: the one of the left is a standard fork for bicycles, it can be noticed how the dimensions are proportional to the size of the wheel needed. In the centre picture, an electric scooter fork is shown. In many cases the fork of a scooter is covered with a non-structural, decorative shroud. The fork at the right is for motorcycles, it can be noticed how its design includes dampers built into the fork.

The picture represented in Figure 5.2.2 shows what the original scooter fork looks like.

*Figure 5.2.2: original fork*

The component is a single piece sheet metal which has been folded to cover three sides. it is properly shaped to adapt to the size of the wheel and its axle. Attached on top is a tube which is connected to the stem.

The fork sees the force directly transmitted by the wheel through its axle.

The original component's material is aluminum. Is it the same alloy used for the steering as seen previously. Its properties are shown in table 5.1.1 on page 24.

A static analysis was computed on the part. The load was halved in order to be distributed on the two channels that the axle mounts to. The force, as already discussed in the previous chapter, has a magnitude of 400 N and it is inclined by 33° from the horizontal plane. Thus, a 200 N force with an inclination of 33° was applied to each of the mounting points. The stem attachment point on the crown was fully constrained. Once the system was defined the analysis was computed using a 3mm mesh.

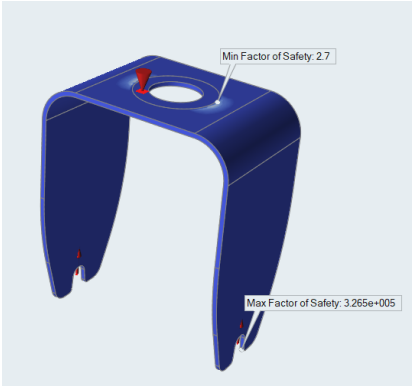


*Figure 5.2.3: original component analysis*

The analysis yielded a result with a minimum safety factor of 2.7 where the constraint was set.

Before starting the design for additive manufacturing, different concepts for the fork were considered.

*Figure 5.2.4: spring/damping systems*

Referring to Figure 5.2.4, he first image from the left is the most common design for electric scooters and is very similar to our original component concept. It consists of the two flat side supports and a small crown. A damping spring is mounted above the crown. The second from the left has two rods, each with a springs and has a larger crown. This design has more damping ability with respect to the first. The third from the right is a more complex suspension system where, in between the two endings of the fork, there is a damper. The last image shows a fork that is made of two arms which are connected to a rotational spring/damper system, built into the joint.

It was decided to keep the original, spring/dampener free system because, as the expectation of this study is to design a middle range city scooter.

The original component's weight is 0.3 kg.

## 5.2.1 Component preparation

The design space and non-design space for the fork are somewhat limited because of the presence of other elements which cannot be modified or moved.
The design space volume was created considering a minimum clearance of 4 mm from the wheel. It was deemed unnecessary to extend the volume below the level of the axle. The dimensions of the design space volume was ultimately set to be 17x16x9cm (height, base, width). In previous iterations a thicker wall was created but after a few cycles of optimisation it was reduced to its shown value. This decision was made because it was not structurally necessary to expand the component laterally and for aesthetic and aerodynamic reasons it was better to have a streamline component. The thickness of the crown's design space needed to be limited because it is delimited by the wheel below and the spring and frame above.

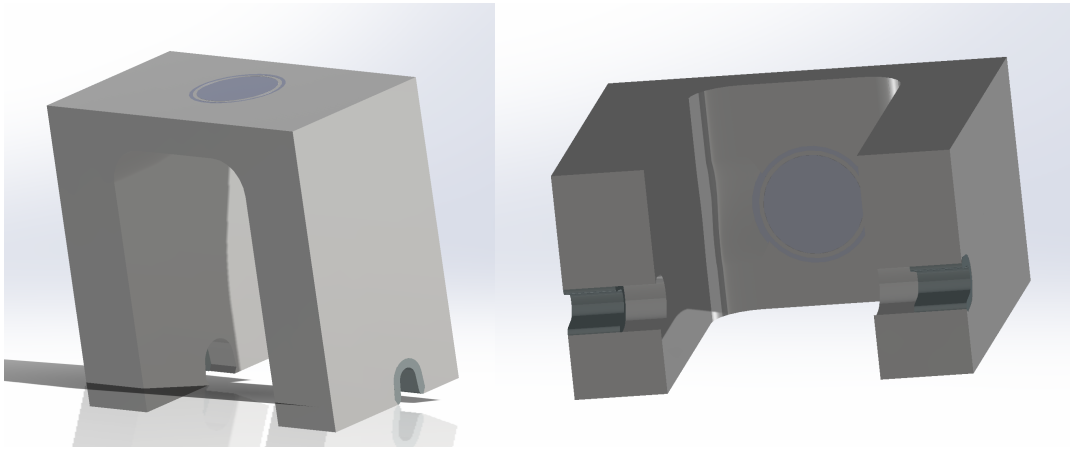

*Figure 5.2.5: design and non design space of the fork*

The exclusion of an upper “stem mounting” tube from the design space comes from the lack of needing to print such a geometry. It is much cheaper to obtain a tube using a standard extrusion process and affix it to the fork after printing. The purpose of this design is to modify only the lower part of the fork. Moreover, it is likely that the original component’s fork and tube were also produced separately and later welded.

The non-design space was set in three areas. On the top of the component, there is a circular ring which is the portion that will be connected to the tube. The thickness of the ring is 2 mm and has the same internal diameter as the stem. This is a slight change from the original design in that the wall thickness was reduced. The internal diameter has to respect the dimensions of the batteries, which are intended to be inserted in the stem. The battery is a package composed of many units which each have a diameter of 18 mm. Each cell is 65 mm long. The battery package was designed so that 3 cells are kept together in parallel so the 44 mm internal diameter could not be changed. The stem’s original external diameter is 56 mm but was progressively reduced to 48 mm.  Static analysis was computed on the ring iteratively by reducing the OD by 2mm each iteration.

The other two areas of the non-design space were set at the bottom of the component where the fork attaches with the axle. For this purpose, two U shaped parts were created on the lateral parts of the fork.

## 5.2.2 Material selection

The materials research for this component was slightly different from the previous part because of the higher stresses the component undergoes. Although the requirements for the material properties are stricter, many of the same considerations explained in the steering section were made. Because of this, the decision fell on AlSi10Mg, the same aluminum alloy selected for the steering, and 10% Kevlar reinforced Onyx. The reasons for this polymer selection will be apparent in the following sections. Another class of materials explored was a specific steel alloy.

AlSi316l is an iron based stainless steel which is resistant to corrosion. It is used in many fields such as jewellery, eye glasses and functional electronic elements, but also used in industrial plants for automotive and aerospace. It is used in SLM technology.

The properties for AlSi316l are shown below in Table 5.2.1.

*Table 5.2.1 - AlSi316l properties*

| ρ (kg/s) | E (GPa) | $\sigma_{ts}$ (MPa) | $\sigma_{ys}$ (MPa) | $\epsilon$ (%) |
|---|---|---|---|---|
| 7.9 | 200 | 529 | 330 | 63 |

The properties of the other materials are shown in the other tables 5.1.2 and 5.1.3 in chapter 5.1.2, pages 27 and 28.

## 5.2.3 Topological optimisation

The model could then be loaded into the optimisation software. As shown in the picture below the loads and constraints are the same used for the analysis of the original component: the force is split in two and distributed on the small lateral parts that contain the axle. The magnitude on each axel mount 200 N and is inclined by 33° from the horizontal. The full constraint is set on the top part of the non-design-space ring.

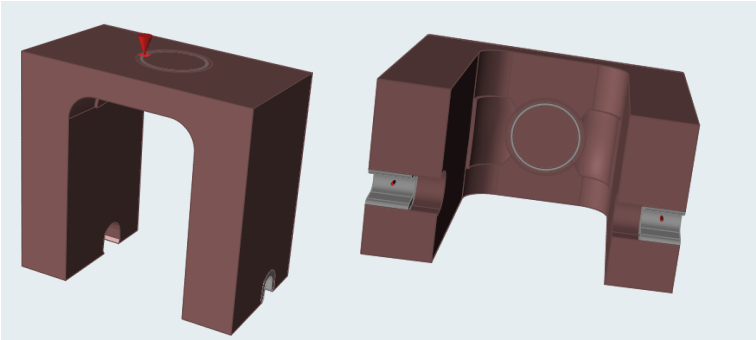

*Figure 5.2.6: fork loads and constraints*

The AlSi10Mg aluminum alloy was considered first. The setting for the topological optimisation, at the beginning, was to maximise stiffness and aimed at a mass reduction of 80%. As with the steering, the mass reduction target was probably way too aggressive for this case.

After a few iterations using the maximise stiffness option, it was decided to switch to the minimisation of the mass. Using this function, a minimum safety factor of 2 was chosen.

After each iteration, it was necessary to “add” mass to the optimisation software in order to obtain a satisfactory result. This mass addition is a function provided by the optimisation software that forces it to add more or less mass than what the software thinks it needs.
This manual iteration was necessary because, unfortunately, the safety factor results of the FE model did not match the FEM analysis results of the reconstructed solid model. At times this method may turn out to be a lengthy process.

The FE model was used as a base to create the solid model with the PolyNurbs tool.

The same process was made for the AlSi316l model, the shape obtained is very similar to the AlSi10Mg one, except slightly thiner. It was discarded because of the excessive weight.

For what concerns the 10% Kevlar reinforced Onyx model, once the solid part was created, the analysis showed too high stresses on the top part at the attachment with the cylindrical part.
The solid was edited by progressively extending and thickening the crown. The process ended when the analysis showed a safety factor higher than 2.

## 5.2.4 Final design

The AlSi10Mg final model is shown in Figure 5.2.7. It weights 0.175 kg and has a minimum safety factor of 4. The mass reduction obtained is the 41%.
The model was finalised in NX in order to round the intersecting parts of the lateral arms with the ring and the two U shaped ends.

*Figure 5.2.7: fork final design*

The 10% kevlar reinforced model's final weight is 0.079 kg. The minimum safety factor is 2.2. The mass reduction is 73%.

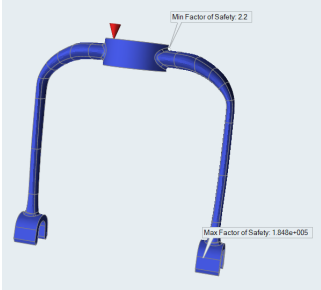


*Figure 5.2.8: final fork design stress analysis*

The following step was needed to find a joint to connect the fork to the tube.
For the aluminum model a simple welding process is the most efficient solution.
For the polymer model a flange was used to fix the tube and the fork. An example is shown below in Figure 5.2.9.

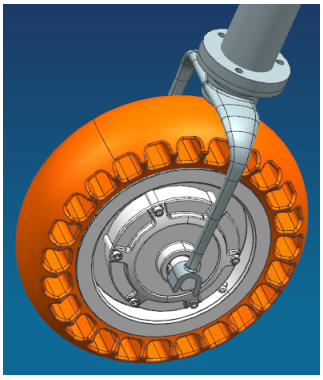

*Figure 5.2.9: fork joint design*

At the end of the design, the component is brought back to the CAD software together with the scooter assembly to make sure it does not collide and has a minimum safety distance from the other components. This checks step was not made for the steering because it is not delimited by other components.

## 5.2.5 Process analysis

Now that the component had finished geometric design, it needed to undergo printing process analysis. First, the metal model was analysed but uploading the solid model to Netfabb where the software suggested the printing orientations shown below in Figure 5.2.10.

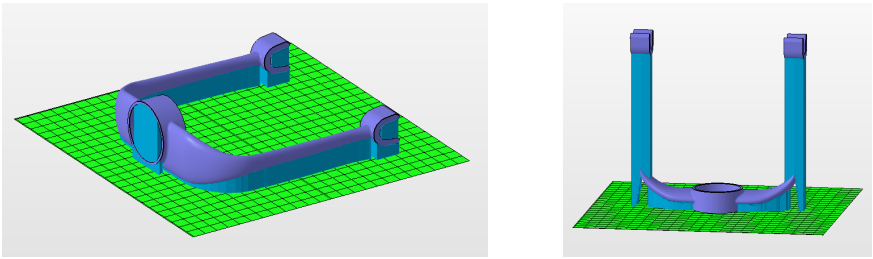

*Figure 5.2.10: possible orientations and supports*

The arrangement shown on the left, the support volume is 55.22 $cm^3$, with a supported area of 41.72 $cm^2$. Shown on the right, there is a support volume of 65.36 $cm^3$ and a supported area of 41.00 $cm^2$. The values are quite similar, but in the second option the are no supports inside the hole which constitutes a benefit. This is beneficial because the removal of support structure is particularly difficult in holes and usually requires post processing to smooth the surface.
As previously mentioned, the critical angle was set at 39° with the non critical angle at 42°. It can be noticed how the largest amount of the supports were generated to support the two protruding ends of the component. The solid model can be edited in order to prevent the necessity of printing supports. This is done by ensuring no part of the part exceeds the non critical angle of 42°. This was done to the part in question by creating an inverted pyramidal shape that connects the two mounting ends with the arms. This can be seen below in figure 5.2.11.

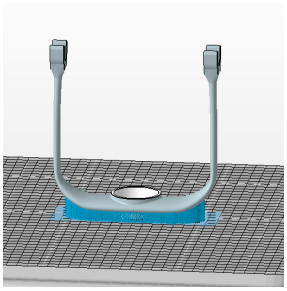

*Figure 5.2.11: edit #1 for support reduction*

This modification made a significant reduction to the volume of the supports. The modified part support volume resulted to be 3.77 $cm^3$, much smaller compared against the previous 55.22 $cm^3$.
A further edit was made to reduce the supports at the crown. The same principle was used, the edges of the crown were connected to top of the cylinder using an angle higher than 42°. The result is shown in the picture below. The new mass is 0.192 kg, the support volume is 1.67 $cm^3$.

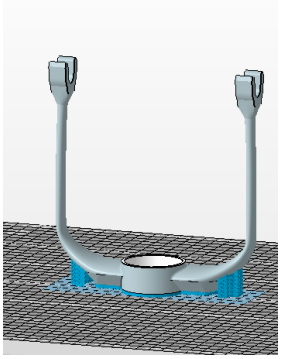

*Figure 5.2.12: edit #2 for support reduction*

The primary difference between the optimised aluminum and plastic components was a thicker crown in the case of the plastic part. However, while optimising for efficient printing, the crown of the aluminum part needed to be thickened. The result was two nearly identical parts, and the plastic design was adapted for both designs.

The arrangement in the machine is favourable because of the limited surface occupied by the part.
In the SLM machine (EOS M 400) the organisation is shown in Figure 5.2.13:

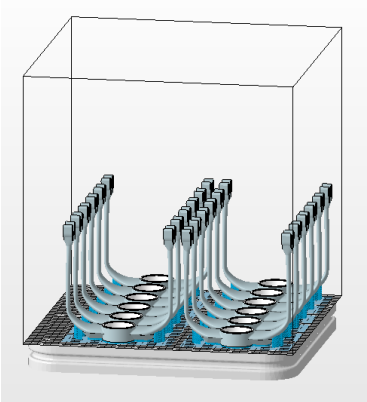

*Figure 5.2.13: arrangement in EOS M400*

12 parts are organised in two rows of 6, with a spacing of 4 mm between the rows.
The amount of AlSi10Mg needed for the job is 400 mm x 400 mm x 168.5 mm (height of the component + 1 mm first layer) = 26.96 $dm^3$. The amount of powder needed is kilogram is 71.44.

The CFF machine suites 7 components, of which 6 are arranged in a row and the last one perpendicular to the the other ones, located laterally.

# 5.3 Truck

The truck is a component used to align two parallel wheels, commonly installed in skateboards.
The truck is composed of two parts: the top part is attached to the bottom of the frame (in the case of the scooter, otherwise for the skateboards it is attached to the deck) and it is called the baseplate; the second part, located in the bottom, is called the hanger. The hanger is the component that contains the wheels and their axels. Connecting the baseplate and hanger are two components: a bushing and kingpin set, and a pivot. The bushing and kingpin is simply a bolt enveloped by a rubber bushing. The stiffness of the truck can be adjusted by tightening a bolt on the kingpin. The pivot is a mechanism resembling a ball and socket mechanism where the hanger would be the ball and the baseplate, the socket. Its purpose is to allow free rotation in all directions while holding the point in place.

*Figure 5.3.1: common truck*

The reason a truck is needed in our electric scooter is that, in order to solve stability issues, the original design requires a three wheel scooter: one in the front and two in the back.
The aid of a truck is necessary in order to keep the wheels parallel, but at the same time, allow some amount of rotation of the frame while turning.

The truck is usually made of metallic material, depending on the model, it can be steel or aluminum. When steel is used, a low strength alloy is commonly preferred.

The production technique mostly used is die casting or gravity casting. Metal casting is the process of depositing a molten metal into a mould. Die casting involves a process that pressurises said molten metal, whereas gravity does not use any outside force/pressure.

Our original component's materials is a 4140 steel. The properties are shown in the table 5.3.1.

*Table 5.3.1 - 4140 steel properties*

| ρ (kg/s) | E (GPa) | $\sigma_{ts}$ (MPa) | $\sigma_{ys}$ (MPa) | $\epsilon$ (%) |
|---|---|---|---|---|
| 7.85 | 190-210 | 655 | 415 | 25.7 |

This steel alloy contains chromium, molybdenum and manganese. It presents high fatigue strength, very good impact and abrasions resistance, high torsional strength and toughness.

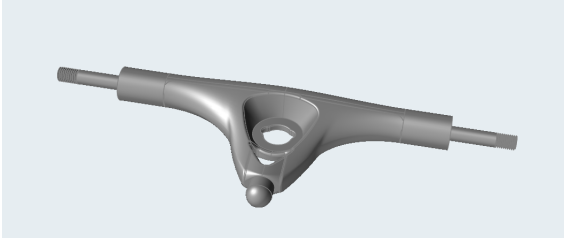

*Figure 5.3.2: original truck hanger*

The design process, in this case, will only focus on the hanger. The original component is shown in Figure 5.3.2.

Let us now focus on the stresses acting on the component.
So far, with the steering and the fork, only the forces acting on the front wheel were needed to proceed with the design. Here we need the forces transmitted to the rear wheels.

In “Product overview” it was explained that the force acting in the back wheel has an inclination of 37° from the horizontal plane, with a magnitude of 660 N. The force will be transmitted to the axle directly from the wheel, so it will maintain the same magnitude and angle (acting on the axle). The force was calculated assuming an impact on one wheel. In this case, however, there are two wheels. To resolve this difference in systems, the impact force is assumed to be distributed between the two wheels. This is the worst case situation of hitting a bump on both wheels rather than just one and results in a force per wheel 330 N.

These calculated forces and impact angles were then used to run analysis of the original component. The system was set up in Inspire and the forces were applied to each ends of the axle. The kingpin/ bushing mount was fully constrained and the pivot was constrained only to allow rotational movement.
The Inspire analysis tool gave an error with the settings above. Many attempts were made, by slightly editing the FE model, the CAD model, and the way the constraints and load were being applied. Despite these changes, an error was still given as result. At this point it was decided to switch the forces and the constraints.
The new analysis settings saw two full constraints at the two ends of the axle; and a unique force of 660 N acting where the kingpin is supposed to be inserted.
The analysis was computed with a 1 mm mesh.
The result is a strong part with a minimum safety factor of 2.5 where there is a sudden change of a diameter between the axle and the hanger which envelops the axle.

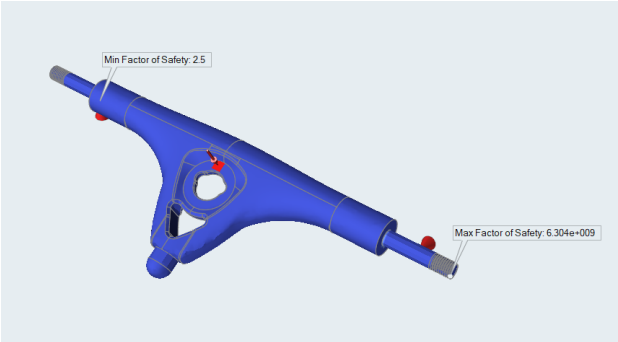


*Figure 5.3.3: truck stress analysis*

The mass of the original component is 0.660 kg.

### 5.3.1 Component preparation

As already mentioned in the previous sections, in order to have the component ready for the optimisation, a volume was created to delimit the areas where the material can be distributed.

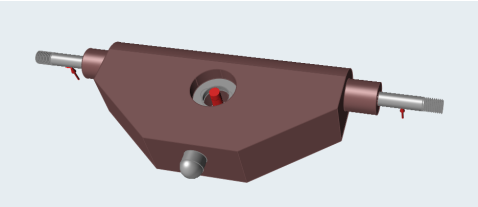

*Figure 5.3.4: truck design and non design spaces*

As shown in Figure 5.3.4, the shape follows the original one, but it was made thicker and more linear. Some parts remained unchanged because they have to match other components. These are the two ends of the axle, the pivot and the ring in which the kingpin is inserted, the thickness of the ring is 8 mm.

From the volume block, two cylinders extend towards the same direction as the axle, for 2 cm, with a diameter of 2 cm.
On the side of the pivot, the block is cut so that material does not cover the joint area. It extends for 5 cm and at the end it turns into an opening V shape where it is cut perpendicularly from the axle direction.

The design space is the red part in the picture. The non design space, the grey parts, are the pivots, the ring surrounding the kingpin and the ends of the axle.

After a first attempt of optimisation using the model described before, it was noticed that the software was not properly distributing the material where the axle is supposed to be. It was then decided to edit the non design part by connecting the two ends of the axle in just one

whole part and subsequently the design space was edited by subtracting the new non design part.

## 5.3.2 Material selection

As previously mentioned, the materials commonly selected for truck are either steel or aluminum. Other classes of materials can be used in more specific cases such as titanium.

For the same reasons as the previous components, the choice fell on AlSi316l, AlSi10Mg and 10% Kevlar reinforced Onyx. The three different families of materials allow us to see the different behaviour and later chose the most proper one. These materials properties are shown in the tables 5.1.2 and 5.1.3 in chapter 5.1.2, pages 27 and 28.

## 5.3.3 Topological optimisation

The solid is now ready to undergo the topological optimisation process.
So far, the other components were optimised with the setting aiming at minimising the mass, this time, the purpose, together with the mass reduction, is to make the part more stiff (there is no need for the truck to be flexible).

For each of the three materials chosen, many attempts of optimisations were made.

The first material is AlSI316l. The loads were first put at an angle of 37° on both sides of the axle. A full constraint was set at the kingpin hole. It would have been proper to add a partial constraint to the pivot, but the software did not allow this operation. This issue probably was given by the geometry of the pivot, which is geometrically similar to a dome on top of a cylinder.
The settings for the topological optimisation are maximise stiffness by keeping the 20% of the mass.
The result of this first attempt was a very thin and linear connection between the axle and the ring that surrounds the kingpin. Because the pivot was left without a constraint, no material was added so that there would be a connection with the rest of the structure. Even though the geometry suggested by the software did not seem to be proper for the purpose of the component, it was decided to create the solid model and manually add two beams which could connect the pivot to the rest of the component.
A static analysis was computed on the new solid model, with a mesh of 1 mm and by setting the load at the kingpin and constraints at the wheels (inverted for the same reason as before). The analysis showed a failure around the midpoint of the material enveloping the axle, the tension stresses were too high and the minimum safety factor in that area was 0.6.
At this point, another attempt was made by keeping the same as option as before (maximise stiffness) but opting for a lower mass reduction, this time a 75%.
The geometry that resulted was of the same shape, just slightly thicker.
Once again, a set of arms were added to connect the pivot to the rest of the part.

The iteration went on until the results of the analysis were satisfying (safety factor higher than 2). The final cycle saw a reduction of 70% of mass in the settings, but with consecutive adjustments to the thickness.
Attention had to be paid in particular to the thickness of the arms to avoid collision with the other components. This issue should be avoided in the first place when the design space is created, but because some components were manually added, it was checked in order to be sure. In this case a parasolid with the surrounding elements was imported into Inspire to facilitate the positioning and adjustment of the beams.

The same process was made for AlSi10Mg and for 10% kevlar reinforced onyx.
The shape obtained with these two materials were not different from the one obtained with the steel alloy. It was concluded, as in previous components, that the AlSi316l is not beneficial in terms of mass, when compared to the other two materials.

## 5.3.4 Final design

Even though the plastic model seems to be optimal, both the 10% Kevlar reinforce Onyx and the AlSi10Mg models were kept as possible designs. Not only are the weight and safety factors important, but the evaluation of the production process and overall costs have high influence on the selection of the best design.

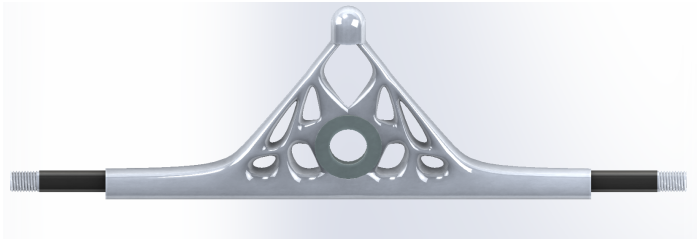

*Figure 5.3.5: truck final design*

The final weight of the AlSi10Mg model is 0.110 kg, resulting in a mass reduction of 83%, compared to a 50% mass reduction for the steel. The minimum safety factor is 1.8 and it corresponds to the variation of diameter where the hanger engages the axle.

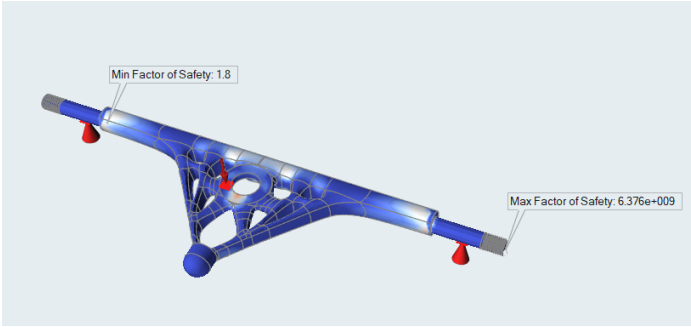


*Figure 5.3.6: truck final design stress analysis*

The weight of the final model obtained with the kevlar-onyx material is 0.035 kg, even though the model is slightly different since it was modified for production difficulties. The editing is explained in the following section.

## 5.3.5 Process analysis

The manufacturing process is now analysed for both the AlSI10Mg and plastic model.

Let us focus on the aluminum model first.

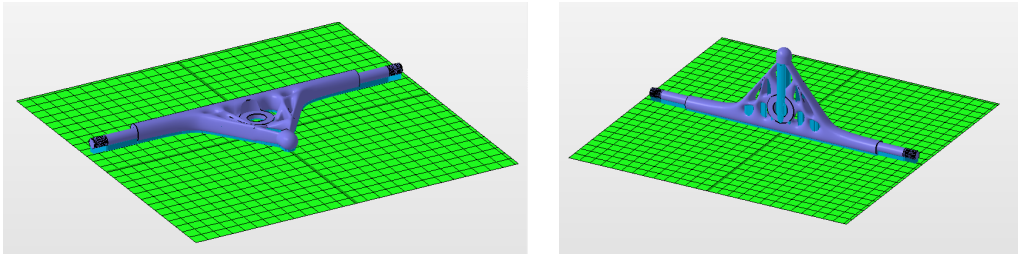

*Figure 5.3.7: truck possible orientations and supports*

In Figure 5.3.7 the arrangement suggested by Netfabb are shown. For the image in the left the support volume would be 4.43 $cm^3$, the area supported 35.82 $cm^2$, whereas for the option at the right the support volume is 6.95 $cm^3$ with 27.26 $cm^2$ of supported area.
The first option seems to be more convenient because support material does not need to be removed from any small holes, unlike the option shown on the right. The problem of support structures in small holes found in the rightmost option be overcome by adding little arms in the middle of the holes. This would make the structure self-supporting or, if not fully self-supporting, would at least reduce the supports needed. Support removal would still be necessary in the main hole where the kingpin is placed. For the pivot area an inclined beam with an inclination higher than 42° could be added for the same purpose. Regardless, the leftmost option is still more convenient because of the lack of supports in the hole and the less material since there is no need for additional beams.

The first option was selected and the supports were generated considering the use of a EOS M 400 machine (it is still being assumed that SLM technology is used when a AlSi10Mg part is being made). After setting a critical angle of 39° and a non critical angle of 42°, the final volume of supports needed for this orientation was 2.26 cm3. The base layer's thickness was set to 1 mm and the laser size to 0.4 mm.

The arrangement in the chamber of the machine is shown in Fig. 5.3.8. The arrangement is automatically generated by the software after the user provides the minimum part spacing and the minimum spacing from the walls. In this case the part spacing was set to 4mm and the wall spacing to 1cm.
This positioning allows the job to have 8 components.
The amount of AlSi10Mg powder needed for the job is 400 mm x 400 mm x 7.5 mm (6.5 mm is the height of the part + 1 mm thickness of the first layer) = 1.2 $dm^3$. The mass of the powder needed is then 3.18 kg.

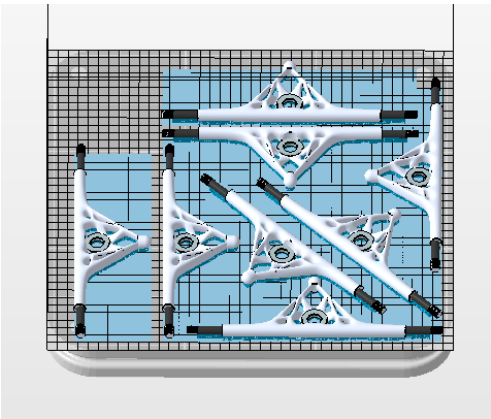

*Figure 5.3.8: arrangement of truck parts in EOS M400*

Concerning the plastic model, it is likely a bad idea to produce the axle in a plastic material like the rest of the hanger. The concern is that the thread section and the section that mates with the wheel's bearing is subjected to wear at a much higher rate with respect to a metalic material. The phenomenon depends on the hardness of the material (330 J/m for Onyx obtained with izod notched test), which, in this case, may not be high enough and could be damaged by the metal bearing of the wheel. Because of this, it was decided to divide the two components and just buy or manufacture a standard axel. As a consequence of this modification, the hanger is now missing the axle and has a hole instead. This structure makes it necessary to change the printing orientation in order to not have supports inside the long hole.

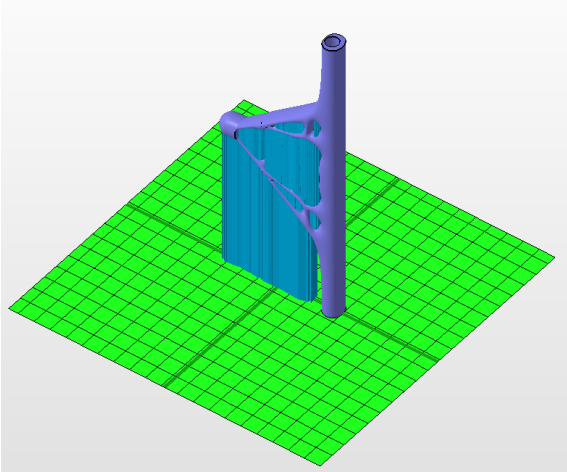

*Figure 5.3.9: polymer truck design orientation and supports*

This orientation leads to a support volume of 47.38 $cm^3$ and 18.06 $cm^2$ of supported surface, assuming the critical angle to be 40° and the non critical angle of 45°. These angled were selected based off of CFF standard angles. As already seen in the case before, the supports going through the holes constitute a problem. In this case, however, it is not as big as a concern as the aluminum case. This is because the supports can be removed in a water based

solution when CFF technologies are used. When there is a large amount of supports that need to be removed, like in this case, it may be opportune to first remove them mechanically and then wait for them to dissolve in the solution.
Another possible solution to overcome the problem is to have the component lay horizontally and, during the printing process when half of the cylindrical part is built, install the axle and wait for the job to finish. This will result in the axel being wrapped in the printing material. This process may be risky because the extruder nozzle head may touch the metallic material if it is not perfectly placed.
Figure 5.3.10 shows the arrangement of the parts in the Markforged machine, it could accomodate up to 34 components.

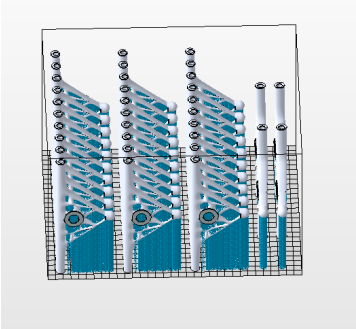

*Figure 5.3.10: arrangement of trucks in Markforged machine*

# 5.4 Frame

The frame is the main structural component of the scooter. It connects the back wheels to the front assembly. In particular, it is connected to the stem with a set of bearings which allow the axial rotation of the stem while keeping the wheel and steering assembly rigidly attached to the frame. In the electric scooter, the frame is also the structure on which the footboard is fixed. This results in it being the part that first accepts the weight force of the user and distributes it the other components.

It differs from the component seen so far for its length and size.
Starting from the front part, it can be described as a ring surrounding the stem, attached to a diagonal, hollow, rectangular cross-sectional arm, about 30 cm long. This cross section ends on a horizontal platform which is made of a rectangular hollow section, about 65 cm long. The platform ends by bending upward at an angle of 20°, extending for 15 cm. At the bottom part of the end of the frame, the plate of the truck is fixed.

The material used for the original component is 6061 aluminum, the same used for the previous components. The material properties can be found in Table 5.1.1 at page 24.

The re-design of this component could lead to a modification on the shape, but not the length, which is a constraint because it has to connect the stem and the wheels.
The dimensions of a box in which the frame could be placed is 90x30x20 cm. In the additive manufacturing industry some machines capable of such volumes can be found, although, they are not common and most of them have drawbacks. Examples of high build volume machines are the LENS 850-R by Optomec, which uses laser deposition technique, but it is mostly used for part repair; EBAM, using electron beam melting principle, but it is still being developed; Stereolitography, but it only makes prototypes; 3D printing Voxel Jet, but it is only used for foundry moulds. Because of the limited availability, it was decided to divide the frame in two components and study them separately, so that they can easily fit in more common machines.
The first part that was analysed was the ring that surrounds the stem and the diagonal segment, the second part was the platform and the part that connects to the truck.

The first step was the static analysis of the two divided components.
In order to compute the analysis, the two components were split on the CAD software, then, to make the analysis more reliable, it was decided to extend both components by 3 cm. This

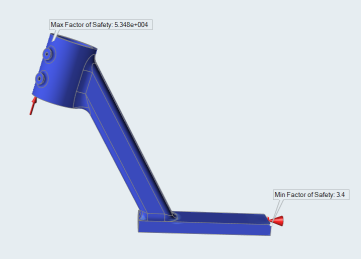

*Figure 5.4.1-a: front facing frame stress analysis*

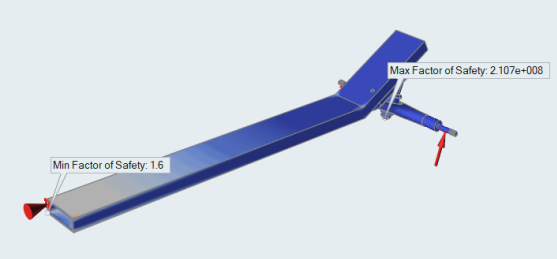


*Figure 5.4.1-b: rear facing frame stress analysis*

decision was made because if the constraint was set too close to a change in direction, like in the case of the diagonal component, it could give incorrect values.

The front facing component undergoes the bump force transmitted by the fork. The magnitude of the force remained the same 400 N and was placed in a direction parallel to stem. The angles and forces are explained in the steering section.
The only constraint (fully constrained) was set in correspondence of where the two parts of the frame would connect. The analysis was ran with a 3 mm mesh and it showed a minimum safety factor of 3.4.

The rear facing component, like the front facing one, undergoes the bump forces transmitted from the back wheels. The worst case scenario of both wheels hitting two bumps at the same time was assumed. The forces are inclined by 37° and have a magnitude of 330 N each. The constraint, similarly to the front facing component, was set where the two sub-components are supposed to attach. The analysis was computed with a 3 mm mesh. It showed a minimum safety factor of 1.6 in correspondence to the constraint.

## 5.4.1 Component preparation

First we are going to see how the diagonal component is prepared for the optimisation.

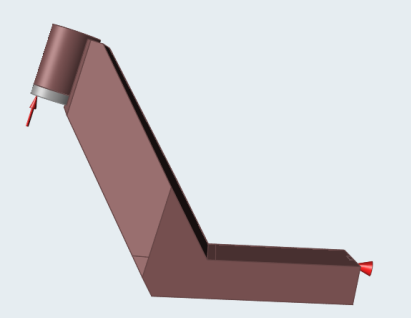

*Figure 5.4.2-a: front facing frame design and non design spaces*

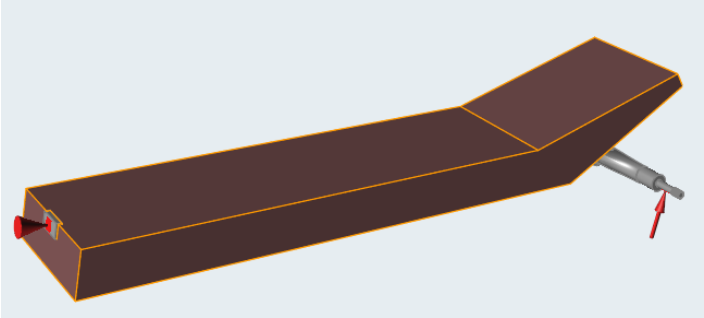

*Figure 5.4.2-b: rear facing frame design and non design spaces*

For the front facing component, very little of the original design remained as "non-design space". The original form was kept as design space, including the same "neck" length and angle, but the whole volume was thickened to allow more design freedom. Part of the ring was transformed into design space. The only non design spaces are the ring that goes on top of the fork spring, and a little box which was needed to create continuity and to put constraint on non design surface.
The decision of reducing the needed height of the ring comes from the availability of smaller bearings in the market. The original component has a set of dual bearings placed at the top and bottom of the ring. The proper spacing allows them to handle high moments.
If a compact design is needed, stronger single bearings can be found. There is a difference in price but it would follow the line of having a particularly lighter component.

The same methodology was applied to the rear facing component: the design space was obtained by thickening the volume of the original component. The non design space is defined by the truck (which was kept in the component to allow the proper positioning of the loads) and a small box in order to create a mounting point and to place a constrain on the model.

On both components, the thickness of the flat horizontal area could not be extended lower by more than 4 cm. If extended more, the bottom would be too close to the ground.

## 5.4.2 Material selection

For the same reasons explained for the other components, the materials chosen for the two components are AlSi10Mg and 10% Kevlar reinforced Onyx. The materials properties are shown in the tables 5.1.2 and 5.1.3 in chapter 5.1.2, pages 25 and 26.

## 5.4.3 Topological optimisation

Of all the components, the frame ones were the most interesting to design because of their more articulated shape and bigger size.

Let us have a look at the diagonal component first.
Similar to the process covered in the previous chapters, the component had to undergo an iterative cycle. Because the initial analysis showed unnecessarily high safety factors, the component was loaded and set up in the optimisation software. A load of 400 N parallel to the axis of the stem was applied at the bottom part of the ring. The optimisation setting was set as mass minimisation with a minimum safety factor of 1.5.
The shape that came out of the optimisation was a sort of reticulum which connected the ring to box where the constraint was applied.
An initial analysis was computed with the FE model in which an iteration was ran in order to figure out what the proper thickness of the FE model's beams was. This step is necessary so that when the actual solid beams are made as a solid model, the thickness will be the closest to the proper one (the solid beams are made by wrapping the shape of the FE model, so the thickness will depend on the FE model).
Once the proper shape was found for the FE model, the reconstruction of the solid started. After this step, static analysis was computed on the solid model. The first time showed that the beams were too weak to handle the stresses. So another iteration started: the beams were thickened and another analysis was be made.
Some beams were eventually moved and some were added order to have a stronger structure.

The end part of the component, where the constraint was placed, got temporary filled with material but only for analysis purposes. It will be later removed and adapted to be joint together with the matching end of the horizontal component.
The process was first made using AlSi10mg as the elected material and then was repeated using the 10% Kevlar reinforced Onyx. The models obtained with the two different materials are very similar.

The same process was used to develop the horizontal component. As for the analysis, two forces of 330 N were applied to the truck's axle at an angle of 37°. The forces are transmitted through the truck (which shape will not be affected by the software because it is set as a non design space) to the frame, and a constraint was placed where the horizontal component will be connected to the diagonal component. The topological optimisation was ran with the aim of minimising the mass while having a minimum safety factor of 1.5.
The shapes obtained with the optimisation can be described as two parallel arms connected all along their length by beams of different size and inclination. The analysis immediately showed dissatisfying results. After many cycles of reconstruction and modification (by adding beams and thickening the already existing ones) and analysis, it was possible to create a model which could handle the stresses. Despite the positive results, the behaviour close to the constraint will need to be verified in a second analysis together with the other component and their joint.
For this component, the process was made for both AlSi10Mg and 10% Kevlar reinforced Onyx.

## 5.4.4 Final design

The images below (Figure 5.4.3 and Figure 5.4.4) show the final models of the diagonal frame component, for AlSi10Mg (Figure 5.4.3) and for 10% Kevlar reinforced Onyx (Figure 5.4.4).

*Figure 5.4.3: metal front facing frame design*

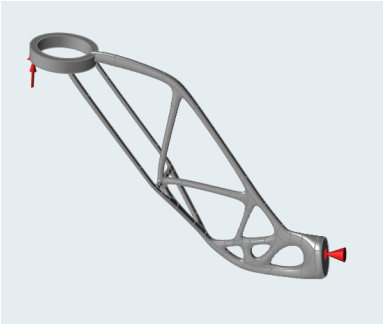

*Figure 5.4.4: polymer front facing frame design*

The AlSi10Mg model weights 0.129 kg, against the 0.790 kg of the original component. The mass reduction achieved is 83%. The minimum safety factor is 1.5 and is located where the constraint is.

The 10% Kevlar reinforced Onyx model's mass is 0.078 kg, yielding in a mass reduction of 90%. The minimum safety factor shown by static analysis is 1.6 in some areas where the direction suddenly changes, towards the constraint.

The rear facing components are shown below in Figure 5.4.5 a and b.
The picture on top (Figure 5.4.5 a) is the final design for the AlSi10Mg horizontal component. Its mass is 0.490 kg (the mass does not include the truck, unlike shown in the figure); the mass

of the original component is 0.570 kg. The mass reduction is 13%. The minimum safety factor found by the analysis is 1.4.

The 10% kevlar reinforced onyx model is shown in the picture below (Figure 5.4.5 b). It has a mass of 0.265 kg. Thus, the mass reduction for this model is 53%. The safety factor is low (around 1.2/1.3) in many areas towards the constraint. It was no longer possible to thicken those areas because of the limit in height of the frame that was discussed at the beginning of the "frame" paragraph.

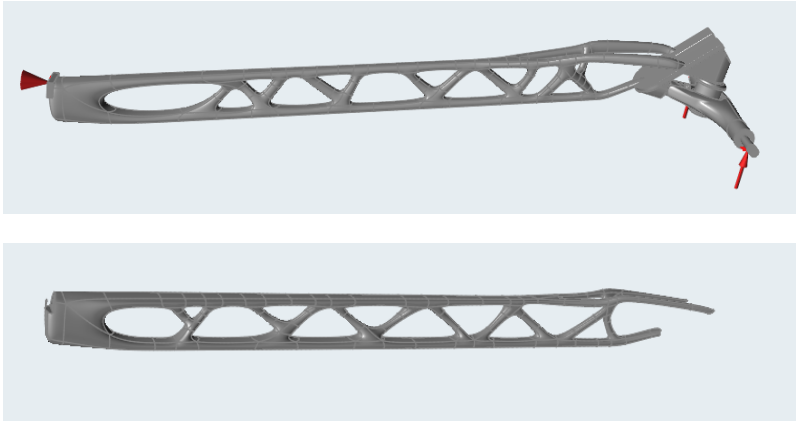

*Figure 5.4.5: a) on top, metal rear facing design*
*b) at the bottom, polymer rear facing design*

## 5.4.5 Process analysis

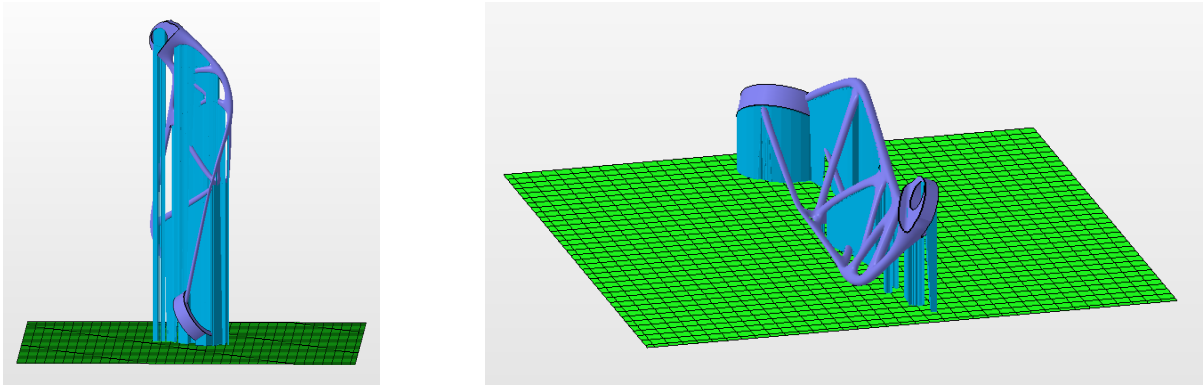

*Figure 5.4.6: possible front facing frame orientations and supports*

The pictures above (Figure 5.4.6) show the orientation suggested by the software Netfabb.

The orientation on the left leads to have a support volume of 99.27 $cm^3$ and a supported area of 22.46 $cm^2$.
The orientation on the right has a volume support of 118.72 $cm^3$ and a supported area of 52.34 $cm^2$.
The option on the left was chosen because of its lower amount of supports and less supported surface.

The image at the left shows the final orientation for the AlSi10Mg design for the SLM machine: EOS M 400. The supports were generated assuming a critical angel of 39° and a non critical angle of 42°. The first layer of support is 1 mm thick. The amount of powder needed for the job is 400 mm x 400 mm x 380 mm (height of the part + 1 mm for the first layer) = 60.8 $dm^3$. The amount in mass is 161.12 kg.
The amount of supports for this component should not be neglected when choosing a design over another one. It must be remembered that, in the case of SLM, the same material is used for both the part and the supports The powders are expensive and the supports are wasted once they are removed and cannot be recovered or reused. So if the volume of the support is higher than that of the part, it may not be worth to use the design, or the part should be edited in order to better suite the production process.

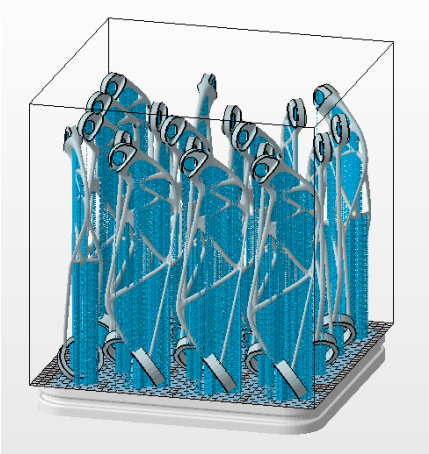

*Figure 5.4.7: arrangement of front facing frame parts in EOS M 400*

The same orientation is not suitable for the plastic model because of the height exceeding the dimension available for the CFF machine (200 mm). As an alternative the second orientation is chosen.

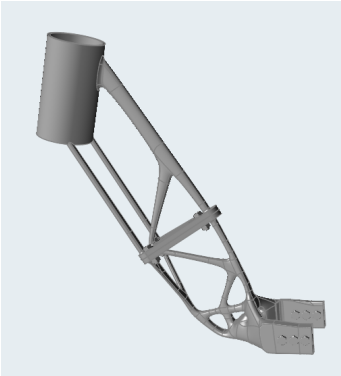

*Figure 5.4.8: possible front facing frame division and joint solution*

Splitting the part into two additional components could also be an option which is explored below.
The component was split in half by creating a flange with mounting holes. The reason for the particular shape at the bottom end of the part will be explained later in the chapter.
In can be noticed in Figure 5.4.8 that the dimension of the ring is the same of the original one, this can be explained as a parallel design that was being developed in that case that the dual bearing assembly is chosen. In this case, the scope of the image is to show the division of the component and the creation of the flange. The design with the extended mounting ring will not be chosen.

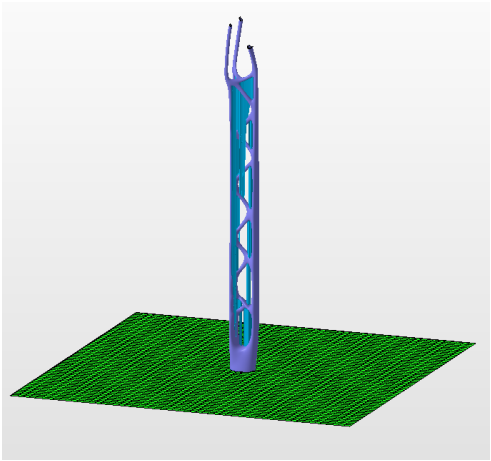

*Figure 5.4.9: possible rear facing frame orientation and supports*

The rear facing part of the frame's best orientation is the one shown in Figure 5.4.9. This orientation may not be compatible with most machines; usually the height of the build volume does not exceed 400mm. This orientation would have a support volume of 43.21 $cm^3$ and a supported area of 9 $cm^2$. An alternative could be changing the orientation in order to have the component fit in the chamber, although, a diagonal orientation (the one that would balance surface and height) would lead to a much higher use of support material.

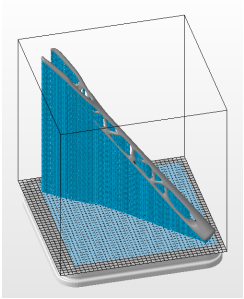

*Figure 5.4.10: rear facing frame arrangement in EOS M 400*

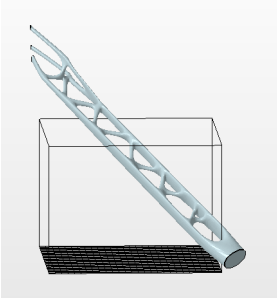

*Figure 5.4.11: rear facing frame arrangement in Markforged machine*

For example, the orientation shown in the left image (Figure 5.4.10) allows the component to fit in the EOS M 400, but the volume of the supports would be 185.09 $cm^3$.

The part does not fit in the Markforged machine by a large margin, as shown at the image at the right (Figure 5.4.11).

The solutions for hypothetical joints are shown below in Figure 5.4.12, they are just a sketch for an example.

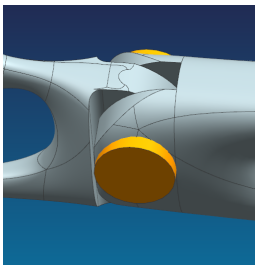

*Figure 5.4.12: joint solution for front and rear facing frames*

This joint provides the rotation of the diagonal segment together with the front part of the scooter about the orange cylinder, to allow the folding of the product. The folding is a design requirement, it was not important for the scope of the thesis but it was considered when a solution for the joint was studied. A blocking mechanism (possibly created by a pin) would prevent the two component to reciprocally move. The activation would be provided by a button that disengages the blocking pin.

The reason why the optimised horizontal component cannot be used in the product will be explained later in the “Cost analysis” chapter. Because of this decision another kind of joint was designed to provide stability for the front facing optimised design and the original horizontal component.

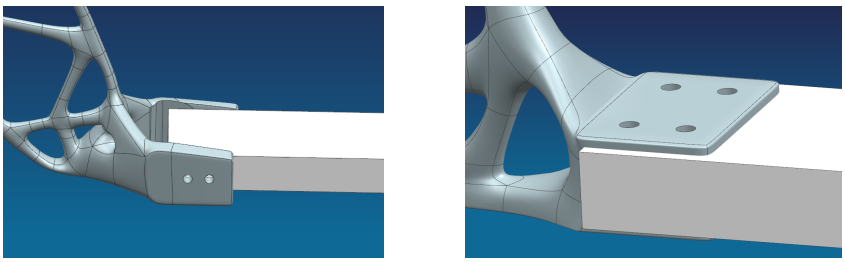

*Figure 5.4.13: possible joint designs for optimised front facing frame and original rear facing frame*

# 6 Cost Analysis

In this paragraph, the costs for manufacturing and other sources of expenses are discussed. First the costs are divided in groups: materials, manufacturing, post processing.

The cost of the materials depends on the purchase price of the material needed to build the component. The price range varies depending on the materials used for each component. Specifically for the components studied, the costs will depend on if AlSi10Mg powder, Onyx spool, Kevlar spool, or AlSi316l powder was used.
The price for each material differs from supplier to supplier (except for Onyx which is exclusively supplied by Markforged). For the purpose of the study, a small price range based off of different suppliers will be sufficient for some of the materials.
Starting with a price between 40€ and 50€ per kilogram of AlSi10Mg powder, an average of 45€ will be used for the calculations. The same price range was found for the steel alloy AlSi316l.
On the Markforged website, in the shop section, all the filament spools prices can be found. The price for Onyx is 190$ for a spool which corresponds to 800$cm^3$. The density of Onyx which was provided by the company's material data sheet, is 1.2 g/cm3 and the price per cm3 is 0.237$, so the price per kilogram is 198$. Converted to euros that is about 167€. The cost of Onyx is then 167€/kg.
The price for the Kevlar filament spools (sold by Markforged) is 300$ for 150$cm^3$. Using the same reasoning made for Onyx, considering that the density of Kevlar is 1.2 g/$cm^3$, the cost of Kevlar is 1406 €/kg.
Considering that the ratio of Kevlar/Onyx for the components was decided to be approximately 1 to 10, the cost for the composite material is 291€/kg.
Concerning the metal components, which will be produced with SLM technology, the cost of the material will apply to both the part and the supports. The parts produced with the CFF Markforged machine will use the materials they were designed with (like the Kevlar reinforced Onyx, but the supports will be made with pure Onyx.

The manufacturing costs vary from technology to technology. Obviously the manufacturing costs will be much higher if the components are produced by a third party. In this case, the parts produced with metal materials will be considered to be produced outside of the company. The price for processing metal powder with SLM technology ranges from 100 to 120€/h, so the average value of 110€/h will be assumed. In order to calculate the time it takes to the machine to build a part, the print speed capacity is needed. For the EOS M 400 machine it was assumed to be capable of creating parts at a rate of 107 cm3/h.
As previously mentioned, it was assumed that the polymeric components would be produced internally by the company with the Markforged machine. The cost for the use of the CFF machine can be assumed to be 2€/h, basically just the cost for the electric power. The printing capacity is approximately 12 $cm^3$/h.

The post processing and finishing operations also have a cost. It is harder to quantify this cost because it depends greatly from case to case. An example of post processing would be support removal, which is very frequently needed in this case. Some of the components may need additional surface finishing when they have holes or mating surfaces. Because of the case-by-case nature of this aspect, the cost of this processing is excluded from the analysis.

Let's now evaluate the cost for each component.

Starting with the steering, there are two designs, the metal one and the polymer one.
The aluminum design shown in Figure 5.1.11, as previously mentioned, is printed without handles. The plastic design will be printed by separately printing the arms.
The AlSi10Mg design's mass is 0.330 kg, so the cost for the material is 15€. Considering the volume of the component, 124.5 cm3, and the print capacity of the machine, the component will be built in 1.16 h. This yields a cost of 128€ for the production. The total cost is 143€. Following the same calculations, the supports, having a mass of 0.002 kg and a volume of 3 cm3, have a material cost of 0.09€ and manufacturing cost of 3€, yielding a total of 3.09€.
The cost for both part and supports is 146.09€.
The mass of the Onyx design is 0.154 kg so the material costs 25.7€. The volume is 128.33 cm3 leading to a the build time of 10.7h, resulting in a cost of 21.4€. The overall cost is 47.1€.
The supports have mass and volume negligible for the cost evaluation.
The actual prices are going to be slightly higher because of the post processing operations. In the case of aluminium they are going to include the support removal and surface finishing. The plastic one needs the same operations. Moreover the handles have to be mounted, and the steering has to be mounted on the stem.
The elevated cost of production of the metal model makes it unreasonable as a product considering that the overall cost for the plastic model is a little above 47€. This cost is still a bit high compared to the cost the same component if it were produced with conventional techniques. For this reason, the component is being considered as an optional "add-on" for the clients who are willing to pay more in order to have a weight reduction and potentially some component customisation.
The plastic model could also be launched with an integrated electric box with different shapes. Here two examples are shown. The blue area on top of the boxes would be the removable cover.

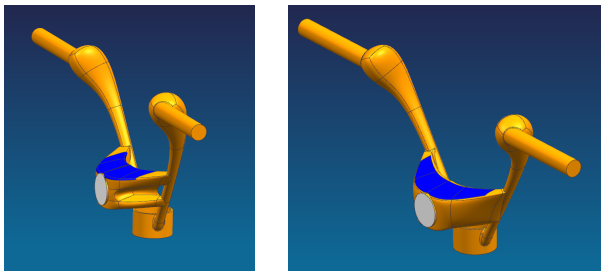

*Figure 6.1: electronic box integration designs*

Let's move on to the next component, the fork.
The evaluation refers to the part which has been modified to reduce the amount of supports and which is outlined in the "Process analysis" section of the truck chapter.
The AlSi10Mg design has a mass of 0.175 kg. With a volume of 65.71 $cm^3$ and a building time of 0.61h, the manufacturing cost is 67.55€ which, added to a material cost of 7.87€, yields a total cost of 75.42€.
The supports, having a mass and volume of respectively 0.004 kg and 1.67 $cm^3$, have a cost of 1.9€.

The onyx-kevlar model's mass is 0.086 kg, its volume is 71.7 $cm^3$. The building time is 5.9h. The total cost is 35€, 23€ of which is for the material and 12€ of which is for manufacturing. The supports mass is 0.002 kg, it has a volume of 1.6 $cm^3$. The cost for the supports is 0.61€. The total cost is 35.61€.
Additional costs are constituted by the support removal, surface finishing and assembly.
In this case, the polymer design seems to be more convenient because it costs less than half of the aluminum part. As for the case of the handle, the price is too high to be mass produced for a standard price range electric scooter. Again, it could be presented as an optional customised component which reduces the weight of the product.

The next component is the truck.
The AlSi10Mg model's mass is 0.110 kg, so the cost for the material is 4.95€. The part has a volume of 41.5 $cm^3$ and a building time of 0.38 h so the manufacturing cost is 42.66€ for a total cost of 47.6€. The supports have a mass of 0.006 kg and a volume of 2.26 $cm^3$, so the cost for the material is 0.27€, the cost for manufacturing is 2.32€. The cost for part and supports together is 50€.
The polymer design has a mass of 0.035 kg, a volume of 42 cm3, takes 3.5 hours for the machine to build the part, so the overall cost is 17.2€. 10.2€ of the 17.2€ constitute the material cost. The supports have a mass of 0.007 kg and a volume of 6 cm3. The build time is 0.5 h, so the overall cost is then 2.17€. The total cost for part and supports is 19.37€.
As for the previous components, additional costs are due to support removal, assembly and surface finish, specifically in the kingpin hole.
Similarly to the other components, the price for the aluminum model is quite high relative to the market; a common aluminum truck produced with die cast or gravity may cost around 20€. The polymer model, instead, has a competitive price considering the important reduction in weight.
The design with a 316l stainless steel could be an even better solution for the future if the binder jetting technology becomes more developed and improved. It would be optimal to have mass produced truck with a low price. Binder jetting does not require the use of supports and does not involve high temperatures because it only uses a bonding material. This makes it much more convenient than the technologies used in this study (SLM and CFF). Unfortunately, it is still a not widely used technology and the materials are not yet proven.

The last component is the frame. First the front facing part of the frame will be discussed.
The aluminum component's mass is 0.129 kg, the cost for the material is 5.8€. The volume of the part is 48.67 $cm^3$, the building time is 0.45 hours. The material cost is 5.8€, the manufacturing cost is 50€, the total cost is 55.8€. The cost for the supports is 12.66€ since its mass and volume are respectively 30g and 11$cm^3$. The total cost of the part and supports is then 68.46€.
The plastic component (produced with CFF technology) has a mass of 0.078 kg, thus having a material cost of 22.4€. Since the part has a a volume of 52.18 $cm^3$, the building time is 4.3 h and the cost for manufacturing is 8.7€, resulting in a total cost of 31.1€.
The supports have a volume of 17.21 $cm^3$, a mass of 0.020 kg, and a building time of 1.43 h so the total cost comes to 6.2€. The total cost of the part is then 37.3€.
The AlSi10Mg rear facing component material cost is 22€, because it has a mass of 0.490 kg. The component's volume is 176.45 $cm^3$, so the building time is 1.6 hours and the manufacturing cost is 181.5€. The overall cost is 203.5€. The cost for the supports is 113€.
The plastic design is not considered since its size is bigger than what could suite the CFF machine.

The rear facing component's cost is too high for the standards of a scooter. The component could be promoted as a particular organic shaped component, but the footboard has to be fixed on top, so it would not even be visible. The original component is thus kept as final design.
The front facing part of the frame has a sustainable cost, but only for the plastic design. 70€ for the aluminum design seems to be too much, moreover the mass reduction is less than the Onyx-Kevlar one.

# 7 Conclusions

Through this study, it was shown that some of the components of an electric scooter can be produced through additive manufacturing technologies and that they pose some advantages when compared to traditional design and manufacturing methods.

The re-designed steering, it was seen, allows to have a reduction of mass up to 87%. With some modifications aiming to improve the aesthetics, the component can be launched into the market as an exclusive ultra-light and good-looking alternative to the standard handlebar.
Customisation is made easy thanks to the additive manufacturing technologies, as seen with the example of the integrated box that was implemented one component with fewer joints and more design freedom. Another way to include customisation could be the addition of a name or symbol imbedded into the part. This is easily addable on the CAD/STL and can be printed normally with no further processes.
Working on the design of the fork, a 73% reduction of mass was achieved. Usually the forks in personal electric scooters are hidden by a plastic cover to improve the aesthetics. In our case if the design is improved from an visual point of view, potentially there would be no need for a cover.
The truck is the component that achieved the highest reduction in mass: 95% with the Kevlar/Onyx design. The 316l design has a mass of only half of the one the original component.
As previously mentioned, this design has a bigger potential in the future, when binder jetting will develop a way to have definitive materials and will be more diffused through the manufacturing industry. Once these developments are made, the component could be made cheaply and could be mass produced.
The frontmost part of the frame contributed to a large reduction, presenting a mass of 1/10 of the original component. Moreover the organic shape might induce interest for its particularity.
The horizontal part of the frame seemed to be less successful than the other components. Nevertheless, in the near future, more machines with bigger work volume may become available and thus could unlock the chance for these kind of large components to be printed. When higher volume machines will be available other solutions for part integration could be studied, such as the production of the whole frame and integration of the plate of the truck.

When using all of the designed in plastic components, the total mass reduction of the scooter is 88%. The optimised components had a mass of 0.424 kg while the standard ones had a mass of 3.65 kg (the calculation was made with the results for the following components: steering, fork, truck, diagonal frame).

The results showed that for all of the components, even though the price for the material is 6 to 7 times higher than the traditional methods, the Kevlar reinforced Onyx material provided better results in terms of mass reduction, yet retained excellent mechanical properties. Of course the assumption that the company owned their own CFF machine had a big impact on the results cost-wise, but since the price of the machine is low enough for it to be considered a reasonable investment for a company who wants to be a step ahead with innovation, it can be considered a reasonable assumption. The same argument could not be made for metal SLM machines because of their much higher price range.

The trends for additive manufacturing technologies and materials are encouraging, and it is expected that the availability of machines and materials will keep growing. The more options there are in the market, the lower the prices will be, and at some point it will become affordable to most people. Companies will be more prone to invest by buying the machines or will simply revolutionise the way they design and produce their products.

# Bibliography

**ARTICLES AND BOOKS**


Andrew N. Dickson, James N. Barry, Kevin A. McDonnell, Denis P. Dowling, *Fabrication of continuous carbon, glass and Kevlar fibre reinforced polymer composites using additive manufacturing,* 2017

Guoying Donga , Yunlong Tanga , Dawei Lib , Yaoyao Fiona Zhao, *Mechanical Properties of Continuous Kevlar Fiber Reinforced Composites Fabricated by Fused Deposition Modeling Process,* 2018

John J. Dunkley, *Metal Powder Atomisation Methods for Modern Manufacturing - Advantages, limitations and new applications for high value powder manufacturing techniques,* 2019

Eric Garner, Helena M.A. Kulken, Charlie C.L. Wang, Amir A. Zadpoor and Jun Wu, *Compatibility in microstructural optimization for additive manufacturing,* 2019

A. Hakan Lava, Ertugrul Bilginb, A. Hilmi Lavb, *A fundamental experimental approach for optimal design of speed bumps,* 2017

Luca Iuliano, *Material from the course "Tecniche di fabbricazione additiva"* Politecnico di Torino, 2019

Arthur J. Petron, *The Folding Roboscooter: Structural Analysis for an Electric Scooter used in Urban Conditions,* 2008

Poukens, Jules, "A classification of cranial implants based on the degree of difficulty in computer design and manufacture". *The International Journal of Medical Robotics and Computer Assisted Surgery,* 2008.

Benjamin K Sovacool, *Early modes of transport in the United States: Lessons for modern energy policymakers,* 2017

"Vranich A., Heritage Science", *Reconstructing ancient architecture at Tiwanaku, Bolivia: the potential and promise of 3D printing,* 2018

Dana Yanocha, Mackenzie Allan, *The electric assist: leveraging e-bikes and e-scooters for more liveable cities,* 2019

A. Zainuddin, K.A.Z. Abidin, I. Ibrahim & M.S. Zakaria, *Stress Analysis of the Personal Electric Vehicle Frame,* 2012

"3D Printed Food System for Long Duration Space Missions".
*sbir.gsfc.nasa.gov*. Retrieved 24 April 2019.

**WEBSITES**

https://www.makeitfrom.com/material-properties/Polyetheretherketone-PEEK

"3D-printed sugar network to help grow artificial liver".
BBC News. 2 July 2012. https://www.bbc.com/news/technology-18677627

Thomas Hart Benton on tour through the States, *Museum uses 3D printing to take fragile maquette,* 2015 | By Alec https://www.3ders.org/articles/20150714-museum-uses-3d-printing-to-take-fragile-maquette-by-thomas-hart-benton-on-tour.html

This meat substitute is printed with a pea and rice protein paste and a 3D printer
Lidia Montes and Qayyah Moynihan, Business Insider España
http://assets.businessinsider.com/this-fake-meat-is-printed-in-a-lab-using-vegetables-and-a-3d-printer-2018-11